A proteolytic complex targets multiple cell wall hydrolases in *Pseudomonas aeruginosa*

Disha Srivastava[1], Jin Seo[1#], Binayak Rimal[2], Sung Joon Kim[3], Andrew J. Darwin[1*]

[1]Department of Microbiology, New York University School of Medicine, New York, New York, United States; [2] Institute of Biomedical Studies, Baylor University, Waco, Texas, United States; [3] Department of Chemistry and Biochemistry, Baylor University, Waco, Texas, United States

* For correspondence: andrew.darwin@med.nyu.edu

[#]Present address: Johnson & Johnson Inc., 199 Grandview Road, Skillman, NJ 08558

Abstract

Carboxy-terminal processing proteases (CTPs) occur in all domains of life. In bacteria, they have been associated with virulence, but their roles are poorly understood. One is the CtpA protease of *Pseudomonas aeruginosa*, which is required for type III secretion system function, and for virulence. Here we show that CtpA works with a previously uncharacterized binding partner to degrade four substrates. The accumulation of at least one of these substrates is required for *ctpA* null mutant phenotypes. All of the substrates are predicted to hydrolyze peptidoglycan cross-links, suggesting that the CtpA complex might be a central control hub for peptidoglycan hydrolysis. When considered with other findings, we propose that this will emerge as a widespread mechanism used by diverse bacteria to control some of their peptidoglycan hydrolases. This is significant, given the links between CTPs and virulence in several pathogens, and the importance of peptidoglycan remodeling to almost all bacterial cells.

Introduction

Pseudomonas aeruginosa is a Gram-negative bacterium that accounts for over 10% of healthcare associated infections with an identifiable cause, and even more in the intensive care unit (Driscoll *et al.*, 2007). It is a versatile pathogen responsible for both acute and chronic infections (Turner *et al.*, 2014). In acute infections, *P. aeruginosa* utilizes a type III secretion system (T3SS) to export proteins into host cells, where they interfere with host cell signaling, immune function, and cause cytotoxicity (Hauser, 2009). In chronic infections, such as those occurring in the lungs of cystic fibrosis

44 patients, *P. aeruginosa* is thought to form biofilms resilient to clearance by antibiotics
45 and the immune response (Wagner & Iglewski, 2008, Clark *et al.*, 2015). Importantly,
46 the emergence of antibiotic resistant strains is increasing, making this pathogen a top
47 priority for the discovery of new therapeutic targets (Moore & Flaws, 2011).

48 Proteases are important for the virulence of many bacterial pathogens. Some *P.*
49 *aeruginosa* proteases are secreted to act on or within host cells, whereas others
50 regulate the virulence characteristics of the bacterial cell itself (Lyczak *et al.*, 2000). One
51 intriguing family of proteases is the carboxy-terminal processing proteases (CTPs),
52 which are found in all three domains of life. CTPs belong to the S41 family of serine
53 proteases with a serine/lysine catalytic dyad (Rawlings *et al.*, 2010). As the name
54 suggests, they are believed to target substrates close to their C-terminus (Hara *et al.*,
55 1991, Keiler *et al.*, 1995). A well described CTP occurs in plant chloroplasts and
56 cyanobacteria, where it cleaves a component of the photosystem II reaction center to
57 process it into its active form (Satoh & Yamamoto, 2007, Che *et al.*, 2013). Gram-
58 negative bacterial CTPs are found exclusively in the periplasmic compartment and have
59 been implicated in cleaving proteins associated with cell envelope function and integrity
60 (Hara *et al.*, 1991, Kumru *et al.*, 2011). Some CTPs have also been associated with
61 virulence, but mostly by poorly defined mechanisms (Mitchell & Minnick, 1997, Bandara
62 *et al.*, 2005, Lad *et al.*, 2007, Bandara *et al.*, 2008, Seo & Darwin, 2013, Carroll *et al.*,
63 2014, Deng *et al.*, 2014). Indeed, despite their widespread conservation, our knowledge
64 of exactly how CTPs function, and which proteins they cleave, is quite limited.

65 The model organism *Escherichia coli* has only one CTP, known as Prc or Tsp
66 (Hara *et al.*, 1991, Keiler *et al.*, 1995). *prc* null mutants have altered cell morphology,

67 increased drug and osmotic sensitivity, and altered virulence (Seoane *et al.*, 1992,
68 Wang *et al.*, 2012). Prc has been proposed to process penicillin binding protein 3
69 (PBP3/FtsI), an essential peptidoglycan transpeptidase required for cell division (Hara
70 *et al.*, 1991). More recently another Prc substrate was discovered, the peptidoglycan
71 hydrolase MepS, which cleaves peptide cross-links between the glycan chains of
72 peptidoglycan (Singh *et al.*, 2012, Singh *et al.*, 2015). These substrates suggest that Prc
73 plays a role in controlling different aspects of peptidoglycan metabolism. However, Prc
74 has also been shown to cleave incorrectly folded polypeptides in the periplasm,
75 suggesting that it is also has a broader role in protein quality control (Silber *et al.*, 1992,
76 Keiler *et al.*, 1995, Keiler *et al.*, 1996).

77 *P. aeruginosa* has a homolog of *E. coli* Prc, with the two proteins sharing over
78 40% amino acid identity and belonging to the CTP-1 subfamily, according to the
79 MEROPS database (Rawlings *et al.*, 2010). In contrast to its role in *E. coli*, *P.*
80 *aeruginosa* Prc has been proposed to degrade mutant forms of the antisigma factor
81 MucA, which occur in strains isolated from cystic fibrosis patients. MucA degradation
82 induces the AlgT/U regulon, causing constitutive production of the exopolysaccharide
83 alginate (Reiling *et al.*, 2005, Sautter *et al.*, 2012). Prc has also been implicated in
84 activating the AlgT/U regulon in strains with a wild type MucA protein (Wood *et al.*,
85 2006). However, Prc has not been shown to cleave any form of MucA directly.

86 Unlike *E. coli* and many other bacteria, *P. aeruginosa* has two CTPs. The
87 second, known as CtpA, is smaller than Prc and in a different subfamily (the CTP-3
88 subfamily; Hoge *et al.*, 2011, Seo & Darwin, 2013). CtpA is required for T3SS function,
89 and a *ctpA* null mutant is less cytotoxic to cultured cells and attenuated in a mouse

90 model of acute pneumonia (Seo & Darwin, 2013). In this study, we have discovered that
91 CtpA forms a complex with an uncharacterized protein, which we have named LbcA
92 (lipoprotein binding partner of CtpA). LbcA is required for CtpA activity *in vivo,* and
93 promotes its activity *in vitro*. We have also identified four substrates of CtpA, all of which
94 are uncharacterized proteins predicted to cleave the peptide cross-links within
95 peptidoglycan. The accumulation of one of these substrates can explain all *ctpA* null
96 mutant phenotypes described so far. We propose that LbcA•CtpA is a proteolytic
97 complex that limits the activity of multiple peptidoglycan hydrolases by degrading them.
98 Based on these and other findings we also argue that many bacterial CTPs might be
99 similarly controlled by partner proteins as part of a widespread mechanism to control
100 peptidoglycan hydrolase activity. This is significant because peptidoglycan cross-link
101 cleavage must be carefully controlled to avoid lethal rupture, but little is known about
102 how this is achieved. Furthermore, there are few molecules more important in bacterial
103 disease, and its treatment, than peptidoglycan.
104
105
106 **Results**
107 **Identification of the CtpA binding partner, LbcA**
108 We modified the chromosomal *ctpA* gene to encode tandem epitope tags at the C-
109 terminus of CtpA (CtpA-FLAG-His_6). This was done in a strain encoding wild type CtpA,
110 and in a strain encoding CtpA with the catalytic serine mutated to alanine (S302A). The
111 rationale was that after tandem affinity purification, substrates might be trapped by the
112 inactive CtpA-S302A version. These experiments were done with or without *in vivo*

113 formaldehyde cross-linking prior to protein purification with nickel agarose followed by
114 anti-FLAG affinity gel. However, the results were similar +/- formaldehyde cross-linking
115 (data not shown) and so only the results from an experiment without cross-linking are
116 shown in Figure 1A.

117 SDS-PAGE revealed that both versions of CtpA co-purified with similar and
118 abundant amounts of a protein running between 50 and 75 kDa markers (Fig. 1A). This
119 protein was identified by mass spectrometry as the uncharacterized PA4667 protein
120 (PAO1 strain designation). A polyclonal antiserum was raised against PA4667 and it
121 confirmed that PA4667 co-purified with the epitope tagged CtpA and CtpA-S302A
122 proteins (Fig 1B). PA4667 is predicted to be an approximately 63 kDa outer membrane
123 lipoprotein with eleven tetratricopeptide (TPR) repeats. The TPR motif is a degenerate
124 34 amino acid sequence that occurs in tandem arrays and mediates protein-protein
125 interactions (Blatch & Lässle, 1999). However, PA4667 does not appear to be a CtpA
126 substrate because its level is similar in *ctpA*$^{+}$ and Δ*ctpA* strains (see below). This is
127 consistent with PA4667 co-purifying equally well with active or inactive CtpA (Fig. 1).
128 Therefore, we will refer to PA4667 as LbcA, (lipoprotein binding partner of CtpA).
129

130 **Δ*lbcA* and Δ*ctpA* mutants have common phenotypes**

131 LbcA interacts with CtpA but it does not appear to be a CtpA substrate. Therefore, we
132 hypothesized that LbcA might be required for CtpA function. Despite repeated attempts
133 we could not construct an Δ*lbcA* in frame deletion mutant. However, we could make
134 Δ*lbcA*::*aacC1* mutants in which most of the *lbcA* gene is replaced by *aacC1*, encoding
135 gentamycin resistance. This was possible only if *aacC1* was in the same orientation as

136 *lbcA*. Global RNA sequencing has shown that *lbcA* is in an operon with the downstream
137 *lolB* and *ipk* genes, which are both essential (Wurtzel *et al.*, 2012). Therefore, we
138 speculate that the *aacC1* promoter helps to express *lolB* and *ipk*, and that our inability to
139 make a Δ*lbcA* in frame deletion might be due to reduced *lolB-ipk* expression (e.g.
140 destabilizing the operon transcript, or removal of an internal promoter within *lbcA*).

141 A Δ*ctpA* mutant has a defective T3SS (Seo & Darwin, 2013). Therefore, we
142 compared the ability of *ctpA* and *lbcA* null mutants to export the T3SS effector proteins
143 ExoS and ExoT into culture supernatants. Both mutants exported less ExoS and ExoT
144 than the wild type (Fig. 2A). The Δ*lbcA::aacC1* phenotype was complemented by an
145 *lbcA*$^+$ plasmid, supporting the contention that it was due to loss of LbcA rather than
146 altered expression of downstream genes. We also complemented the Δ*ctpA* mutation
147 with wild type CtpA but not the proteolytically inactive CtpA-S302A, as shown previously
148 (Fig. 2A; Seo & Darwin, 2013).

149 Recently we have discovered that a Δ*ctpA* null mutant has a phenotype in an
150 assay where bacteria are grown in static liquid culture and then cells attached to the test
151 tube surface are visualized by staining with crystal violet (O'Toole & Kolter, 1998). After
152 an 8 hour incubation, the Δ*ctpA* mutant had attached robustly whereas the wild type had
153 not (Fig. 2B). This appears to be an accelerated surface attachment phenotype because
154 after a 16 hour incubation, the wild type strain caught up so that its surface attachment
155 was indistinguishable from the Δ*ctpA* mutant (data not shown). We tested if the *lbcA* null
156 mutant shares this phenotype and found that it did (Fig. 2B). Furthermore, the Δ*lbcA*
157 and Δ*ctpA* mutants were complemented by plasmids encoding the wild type proteins,
158 but the Δ*ctpA* phenotype was not complemented by CtpA-S302A. All strains grew at

159 similar rates in the conditions used in these assays (data not shown), showing that the
160 accelerated surface attachment of the mutants was not due to faster growth.

161 *ctpA* and *lbcA* null mutants share defective T3SS and accelerated surface
162 attachment phenotypes (Fig. 2). An *lbcA* null mutant is also sensitive to overproduction
163 of a secretin protein, which was the phenotype by which we originally discovered a *ctpA*
164 null mutant (data not shown; Seo & Darwin, 2013). All of these findings support the
165 hypothesis that LbcA might be required for CtpA proteolytic function.

166

167 **Evidence that LbcA recruits CtpA to the outer membrane**

168 If CtpA interacts with LbcA, a predicted outer membrane lipoprotein, then this should
169 tether CtpA to the membrane. However, we and others concluded that CtpA is a soluble
170 periplasmic protein because it was released from cells by osmotic shock (Hoge *et al.*,
171 2011, Seo & Darwin, 2013). Even so, a significant amount of CtpA was not released in
172 our experiment (Seo & Darwin, 2013). Perhaps the harsh osmotic shock can disrupt
173 LbcA•CtpA complexes. Indeed, we have now found that the amount of CtpA released by
174 osmotic shock varies between experiments. However, a significant amount of CtpA is
175 always retained in the spheroplasts, and this is more pronounced when cultures are
176 harvested at a lower optical density (OD) than before (OD 600nm of 1 instead of 1.5;
177 data not shown). Therefore, to address the influence of LbcA, we osmotically shocked
178 *lbcA*$^+$ and Δ*lbcA* strains that had been grown concurrently to OD 600 nm of 1 (Fig. 3A).
179 In the *lbcA*$^+$ strain, most CtpA was not released by osmotic shock, whereas a soluble
180 periplasmic control protein was released completely. However, in the Δ*lbcA* mutant,
181 most CtpA was now released by osmotic shock. This supports the hypothesis that LbcA

182 influences the localization of CtpA, perhaps by tethering it to the outer membrane.

183 To test this further we used an approach that separates cells into soluble and
184 insoluble fractions by French press lysis and ultracentrifugation. Interestingly, LbcA was
185 found in both the soluble and insoluble fractions (Fig. 3B). We do not yet know if this
186 has any physiological significance, or if it might be an artifact resulting from some LbcA
187 disengaging from the membranes during sample processing. Regardless, the important
188 finding is that in an *lbcA*$^+$ strain, CtpA fractionated similarly to LbcA, being distributed
189 between soluble and insoluble fractions. However, in an Δ*lbcA* mutant, CtpA was found
190 only in the soluble fraction (Fig. 3B). Once again, these data are consistent with the
191 LbcA•CtpA interaction serving to localize some CtpA to the outer membrane.

192

193 **Isolation of putative CtpA substrates**

194 All the preceding experiments suggested that CtpA and LbcA form a complex, with both
195 proteins required for CtpA to target its substrates. Therefore, we reasoned that the best
196 approach to search for those substrates would be to purify only the CtpA that is part of a
197 LbcA•CtpA complex. To achieve this, we modified our tandem affinity tag approach by
198 putting the His_6 tag on CtpA or CtpA-S302A, and the FLAG tag on LbcA. The tagged
199 proteins were encoded by separate expression plasmids and produced at near
200 physiological levels as judged by immunoblot (data not shown). To improve the
201 probability of success, the plasmids were introduced into a Δ*ctpA* mutant to increase the
202 abundance of uncleaved substrates in the strain producing the CtpA-S302A-His_6 trap.

203 Strains were grown in T3SS inducing conditions and treated with formaldehyde
204 to covalently cross-link associated proteins. Proteins were purified using nickel agarose

205 followed by anti-FLAG affinity gel, and analyzed by SDS-PAGE and silver staining (Fig.
206 4A). Purification of the LbcA•CtpA complexes was successful, and some proteins
207 appeared to be enriched with LbcA•CtpA-S302A compared to LbcA•CtpA (Fig. 4A). We
208 analyzed two independent purification samples from each strain by mass spectrometry.
209 101 proteins were present in both LbcA•CtpA-S302A samples, but neither of the
210 LbcA•CtpA samples (Fig. 4B and Supplemental Table 1). Most of these were detected
211 in low amounts. However, for our initial follow-up, we focused on the most abundant as
212 judged by peptide spectrum matches (PSMs), the uncharacterized PA0667 protein (Fig.
213 4B). PA0667 has a predicted Sec-dependent signal sequence, a LysM peptidoglycan-
214 binding domain, and an LytM/M23 peptidase domain. It shares these domains with, and
215 is 35% identical to, the *E. coli* MepM protein, a DD-endopeptidase that cleaves the D-
216 Ala-meso-DAP peptide cross-links of peptidoglycan to facilitate cell elongation (Singh,
217 2012). Therefore, we will refer to PA0667 as MepM.
218

219 **Evidence that MepM is a proteolytic substrate of the LbcA•CtpA complex *in vivo***

220 To quickly test if MepM might be an LbcA•CtpA substrate, we constructed a plasmid
221 encoding arabinose inducible MepM-FLAG and introduced it into wild type, Δ*ctpA* and
222 Δ*lbcA* strains. MepM-FLAG synthesis was induced by including 0.02% arabinose in the
223 growth media, and equivalent amounts of each strain were analyzed by anti-FLAG
224 immunoblot. This revealed that MepM-FLAG was undetectable in the wild type strain,
225 whereas it was abundant in Δ*ctpA* and Δ*lbcA* mutants (Fig. 4C). To analyze
226 endogenous MepM we raised a polyclonal antiserum against the purified protein. This
227 antiserum was unable to detect MepM in the wild type strain, but once again it revealed

228 that MepM accumulated in a Δ*ctpA* mutant (Fig. 4D). Furthermore, the accumulation of
229 MepM was reversed by complementing the Δ*ctpA* mutant with a plasmid encoding wild
230 type CtpA, but not by the proteolytically inactive CtpA-S302A (Fig 4D). Together, all of
231 these data support the hypothesis that MepM is cleaved by CtpA *in vivo*, and that this is
232 also dependent on the presence of LbcA.
233
234 **Deletion of *mepM* suppresses Δ*ctpA* mutant phenotypes**
235 If the role of CtpA is to degrade/inactivate MepM, then some or all Δ*ctpA* phenotypes
236 might be caused by MepM accumulation. If so, a Δ*mepM* mutation should suppress
237 those Δ*ctpA* phenotypes. To test this, we introduced a *mepM* in frame deletion mutation
238 into wild type and Δ*ctpA* strains and then surveyed their phenotypes (Fig. 5).
239 First, we monitored the export of ExoS and ExoT into culture supernatants by the
240 T3SS. The Δ*mepM* mutation did not have a strong effect on the amount of ExoS/T in the
241 supernatant, although their levels in the Δ*mepM* mutant were slightly increased
242 compared to wild type, a trend that was consistent in independent experiments (Fig. 5A
243 and data not shown). The Δ*ctpA* mutant exported lower amounts of ExoS/T, as before.
244 However, this phenotype was suppressed by the introduction of a Δ*mepM* mutation,
245 with the ExoS/T secretion profiles of wild type and Δ*ctpA* Δ*mepM* strains being
246 indistinguishable (Fig. 5A). Furthermore, when *mepM* was expressed from a plasmid in
247 the Δ*ctpA* Δ*mepM* mutant it reduced T3SS function (Fig 5A). These data support the
248 hypothesis that the accumulation of MepM was responsible for the defective T3SS
249 phenotype of the Δ*ctpA* mutant.
250 We also investigated cytotoxicity towards CHO-K1 cells by measuring their

251 release of lactate dehydrogenase (LDH) into the cell culture supernatant. This is a well-
252 established model for studying the toxic effect of the *P. aeruginosa* T3SS on eukaryotic
253 cells (Lee *et al.*, 2005). Indeed, we reported previously that a Δ*ctpA* mutant is less
254 cytotoxic towards CHO-KI cells (Seo & Darwin, 2013). Here, we found that the
255 cytotoxicity phenotypes of the Δ*ctpA*, Δ*mepM* and Δ*ctpA* Δ*mepM* strains were fully
256 consistent with their T3SS phenotypes (Figs. 5A and B). Δ*mepM* did not affect
257 cytotoxicity, Δ*ctpA* reduced it, and this reduction was suppressed in the Δ*ctpA* Δ*mepM*
258 double mutant (Fig. 5B). These data further suggest that MepM accumulation in a Δ*ctpA*
259 mutant causes the defective T3SS and the reduced cytotoxicity to CHO-K1 cells.

260 Finally, we tested the effect of the Δ*mepM* mutation in the surface attachment
261 assay. The Δ*mepM* mutation suppressed the accelerated surface attachment phenotype
262 of the Δ*ctpA* mutant, and this suppression could be reversed by the introduction of a
263 *mepM*$^+$ plasmid (Fig. 5C). Therefore, all of these findings suggest that the various
264 phenotypes of a Δ*ctpA* null mutant require MepM. As expected, we have also found that
265 a Δ*mepM* mutation suppresses these same phenotypes of a Δ*lbcA* mutant (data not
266 shown). The simplest explanation for all of this is that the phenotypes of LbcA•CtpA-
267 defective strains are the result of increased hydrolysis of peptidoglycan cross-links,
268 which we tested next.

269

270 **Peptidoglycan cross-linking is reduced in a Δ*ctpA* mutant**

271 The peptidoglycan compositions of wild type and Δ*ctpA* strains were characterized by
272 liquid chromatography-mass spectrometry (LC-MS). The peptidoglycan repeat unit in *P.*
273 *aeruginosa* consists of the disaccharide Glc*N*Ac-Mur*N*Ac with a pentapeptide stem L-

274 Ala-D-iso-Gln-*m*-Dap-D-Ala-D-Ala attached to the lactic moiety of Mur*N*Ac (Fig. 6A). The
275 disaccharides are joined by $\beta_{1\text{-}4}$ glycosidic linkages to form the glycan chain. The glycan
276 chains are cross-linked via a peptide bond between the sidechain of *m*-DAP in an
277 acceptor stem of one repeat unit, to the carbonyl carbon of a penultimate D-Ala in a
278 donor stem of a neighboring glycan chain. To characterize peptidoglycan compositions,
279 isolated cell walls were digested with mutanolysin, which cleaves the $\beta_{1\text{-}4}$ glycosidic
280 linkage between Mur*N*Ac and Glc*N*Ac, resulting in muropeptide fragments with intact
281 cross-links. Muropeptide ions detected by LC-MS were identified by matching the
282 observed m/z values to the corresponding entries in a muropeptide library generated *in*
283 *silico* using an in-house program. Forty-seven unique muropeptide ion species from the
284 wild type, and thirty-three from the Δ*ctpA* mutant were selected for the analysis.
285 Muropeptide fragments were quantified by integrating the extracted ion chromatogram
286 (XIC) of the selected muropeptide ion (Chang *et al.*, 2017a, Chang *et al.*, 2017b, Chang
287 *et al.*, 2017c). The normalized summed integrals of muropeptides from the XIC ion
288 current were categorized based on the cross-link number per muropeptide fragment
289 (Fig. 6B). Muropeptide fragments larger than trimers were not observed, and the most
290 abundant muropeptides were peptidoglycan dimers. Representative mass spectra of
291 monomer, dimer, and trimer from the wild type are shown in Figure 6, and the chemical
292 structure and calculated masses for these selected peptidoglycan monomer, dimer, and
293 trimer are in Supplementary Figure S1.

294 This analysis revealed that the cell walls of the Δ*ctpA* mutant had a reduced
295 concentration of peptidoglycan dimers compared to the wild type (87.30% ± 1.34% and
296 75.85% ± 3.90% for wild type and Δ*ctpA* mutant, respectively; Fig. 6B), and a

297 concomitant increase in monomers. This is consistent with decreased peptidoglycan
298 cross-linking efficiency (ρ_{CL}) in the Δ*ctpA* mutant. The calculated ρ_{CL} for wild type and
299 Δ*ctp*A mutant were 50.86% ± 0.98% and 49.46% ± 0.18%, respectively (Fig. 6C). The
300 reduced peptidoglycan cross-linking in the Δ*ctpA* mutant is small. However, the
301 accompanying increase in trimers and monomers, indicates altered peptidoglycan
302 biosynthesis. Furthermore, a relatively small effect was expected because a *ctpA*
303 mutant grows well, had very few phenotypes in a Biolog Phenotype MicroArray (Seo &
304 Darwin, 2013), and is not notably sensitive to low osmotic conditions (data not shown).
305 Regardless, these data are consistent with the phenotypes of LbcA•CtpA-defective
306 resulting from accumulation of a peptidoglycan cross-link hydrolase.
307

308 **LbcA enhances CtpA-dependent degradation of MepM *in vitro***

309 The *in vivo* experiments suggested that MepM might be a direct proteolytic substrate of
310 CtpA, and that its cleavage also requires LbcA (Fig. 4). To test this, we purified C-
311 terminal hexahistidine tagged versions of CtpA, CtpA-S302A, LbcA and MepM by
312 nickel-agarose affinity chromatography. Equimolar amounts of these proteins were
313 incubated for 3 hours at 37˚C (Fig. 7A). MepM was stable when incubated alone.
314 However, in the presence of CtpA the amount of MepM decreased, suggesting that
315 CtpA had degraded it. Furthermore, when MepM was incubated with both CtpA and
316 LbcA it became undetectable, which is consistent with LbcA enhancing CtpA-dependent
317 degradation (Fig. 7A). Importantly, there was no degradation of MepM when it was
318 incubated with CtpA-S302A alone, or with CtpA-S302A + LbcA. This supports the
319 contention that the S302A mutation destroys CtpA proteolytic activity, that the

320 degradation of MepM was due to CtpA and not a contaminating protease activity, and
321 that LbcA cannot degrade MepM itself. Therefore, these *in vitro* assays support the
322 hypotheses that MepM is a direct substrate of CtpA, and that LbcA enhances the
323 proteolysis.

324 To further test the role of LbcA we monitored the degradation of MepM by CtpA
325 over time, +/- LbcA (Fig. 7B). This demonstrated that the rate of CtpA-dependent
326 degradation of MepM was faster in the presence of LbcA. We also incubated CtpA +/-
327 LbcA with another LytM/M23 peptidase domain protein, PA3787. However, PA3787 was
328 not degraded significantly throughout the time course of the experiment (Fig. 7B). This
329 indicates that CtpA has substrate specificity, even amongst related proteins.

330 These *in vitro* experiments support the characterization of MepM as a direct
331 proteolytic substrate of CtpA. They also suggest that LbcA catalyzes CtpA-dependent
332 proteolysis. This offers an explanation for the requirement of LbcA *in vivo*, and is
333 consistent with Δ*ctpA* and Δ*lbcA* mutants having common phenotypes. CtpA is a
334 member of the C-terminal processing protease family. However, our *in vitro* assays
335 suggest that it degrades MepM rather than only processing its C-terminus in a single
336 cleavage event. We did not observe any stable fragments in the *in vitro* assays, and we
337 also have not detected stable truncated MepM fragments *in vivo* with our MepM
338 antiserum (data not shown). Of course, it remains possible that CtpA cleaves close to
339 the C-terminus of MepM, but that it also cleaves the reaction product(s) in a serious of
340 C-terminal proteolytic events resulting in complete degradation.

341

342

343 **The LbcA•CtpA complex also degrades some other predicted peptidoglycan**
344 **cross-link hydrolases**

345 Based on PSM, the MepM substrate was the most abundant protein that co-purified with
346 the LbcA•CtpA-S302A trap (Fig. 4B). Remarkably, the three proteins with the next
347 highest PSM values are also known or predicted peptidoglycan hydrolases (PA1198,
348 MltD and RlpA). PA1198 belongs to the NlpC/P60 peptidase family and is homologous
349 to *E. coli* MepS (Singh *et al.*, 2012). In *E. coli*, MepS is as DD-endopeptidase involved in
350 cell elongation, and it targets the same peptide cross-links as MepM (Singh *et al.*,
351 2012). MltD (PA1812) and RlpA (PA4000) are lytic transglycosylases that attack the
352 glycan chain of peptidoglycan (Bateman & Bycroft, 2000, Lee *et al.*, 2013). RlpA
353 contributes to maintenance of cell shape, and to daughter cell separation in *P.*
354 *aeruginosa* (Jorgenson *et al.*, 2014).

355 CtpA cleaves one peptidoglycan hydrolase (MepM). Therefore, we considered
356 the possibility that it might cleave the other three that co-purified abundantly with the
357 LbcA•CtpA-S302A complex. To test this, we constructed plasmids encoding arabinose
358 inducible C-terminal FLAG tagged versions of PA1198, MltD and RlpA, and introduced
359 them into wild type and Δ*ctpA* strains. Synthesis of each FLAG-tagged protein was
360 induced with arabinose, and cell lysates were analyzed by anti-FLAG immunoblot. Like
361 MepM-FLAG, PA1198-FLAG was undetectable in the wild type strain, whereas it
362 became abundant in a Δ*ctpA* mutant (Fig. 8A). We extended the analysis for PA1198 to
363 study the effect of an Δ*lbcA* mutation, which also caused PA1198 accumulation (Fig.
364 8A). Therefore, PA1198 behaves the same as MepM, suggesting that is also a
365 substrate of the LbcA•CtpA complex. However, MltD-FLAG and RlpA-FLAG were easily

366 detectible in wild type strains, and did not accumulate in a Δ*ctpA* mutant (Fig. 8A).
367 Although a trivial explanation is possible (e.g. the FLAG tag inhibited cleavage), this
368 suggests that MltD and RlpA are not CtpA proteolytic substrates. An intriguing
369 possibility for their abundant co-purification with the LbcA•CtpA-S302A trap is that they
370 form a complex with one or more CtpA substrates (see Discussion).

371 Two predicted peptidoglycan hydrolases accumulate in Δ*ctpA* and Δ*lbcA*
372 mutants, the LytM/M23 peptidase family member MepM and the NlpC/P60 family
373 member PA1198 (Fig. 8A). Therefore, in addition to the pull down approach to find
374 substrates, we also used a biased approach by screening other putative *P. aeruginosa*
375 peptidoglycan hydrolases. Again, this was done by constructing plasmids encoding
376 arabinose inducible C-terminal FLAG tagged versions. The candidates included three
377 more members of the LytM/M23 peptidase family that MepM is in (PA3787, PA4404 and
378 PA5551), two members of the LytM/M23 family with predicted defective peptidase
379 domains (PA3623/NlpD and PA5363; these dLytM proteins regulate amidases; Uehara
380 *et al.*, 2009, Uehara *et al.*, 2010, Yakhnina *et al.*, 2015), and three more members of the
381 NlpC/P60 family that PA1198 is in (PA0639, PA1199 and PA1844/Tse1). We also
382 tested PA2272 (PBP3A) and PA4418 (PBP3), two homologs of *E. coli* penicillin binding
383 protein 3 (PBP3/FtsI). In *E. coli*, PBP3 was identified as a substrate of its only carboxy-
384 terminal processing protease, Prc/Tsp (Hara *et al.*, 1991). Most of these candidates
385 were present at similar levels in wild type, and Δ*ctpA* strains, suggesting that they are
386 not CtpA substrates (Fig 8A). However, PA1199 and PA4404 were not detected in the
387 wild type but accumulated in the Δ*ctpA* mutant. Again, we extended the analysis for
388 these two proteins to an Δ*lbcA* mutant, and they also accumulated in this strain (Fig.

389 8A). Therefore, the biased approach of screening putative peptidoglycan hydrolases
390 identified two more candidates as putative LbcA•CtpA proteolytic substrates.

391 To test if the PA1198, PA1199 and PA4404 proteins that accumulated in the
392 Δ*ctpA* and Δ*lbcA* mutants are proteolytic substrates, we purified C-terminal
393 hexahistidine tagged versions and tested them *in vitro*. All three were degraded most
394 effectively when incubated with LbcA and CtpA, as we had observed with MepM (Figs.
395 7A and 8B). As expected, there was no degradation when the proteins were incubated
396 with LbcA and CtpA-S302A (Fig. 8B).

397 CtpA degrades four predicted peptidoglycan hydrolases. Two belong to the
398 LytM/M23 peptidase family and are homologous to *E. coli* MepM (PA0677/MepM and
399 PA4404), and two belong to the NlpC/P60 family and are homologous to *E. coli* MepS
400 (PA1198 and PA1199). Significantly, all four are predicted to cleave the same peptide
401 cross-link bonds of peptidoglycan. Breaking these cross-links poses an obvious danger
402 to the bacterial cell. Therefore, the LbcA•CtpA complex might be the central control hub
403 used by *P. aeruginosa* to regulate this activity. Our discovery of multiple substrates also
404 raises an intriguing question. If four or more peptidoglycan hydrolases can accumulate
405 in a Δ*ctpA* mutant, why did removing only one of them (MepM) suppress the
406 phenotypes? Possible explanations are considered in the Discussion.

407

408

409 **Discussion**

410 *P. aeruginosa* CtpA is required for T3SS function, cytotoxicity, and virulence (Seo &
411 Darwin, 2013). Other bacterial CTPs have also been associated with virulence (Baumler

412 *et al.*, 1994, Mitchell & Minnick, 1997, Bandara *et al.*, 2005, Lad *et al.*, 2007, Bandara *et*
413 *al.*, 2008, Hernandez *et al.*, 2013, Carroll *et al.*, 2014, Deng *et al.*, 2014). However, in
414 most cases the mechanisms remain largely unexplored, and very few CTP substrates
415 have been identified. Our goal was to address this deficiency for CtpA in *P. aeruginosa*.
416 We discovered that CtpA forms a complex with an uncharacterized outer membrane
417 lipoprotein, LbcA, and that both proteins are required for CtpA-mediated proteolysis *in*
418 *vivo* and *in vitro*. We also identified four substrates of this complex, all of which are
419 predicted to be hydrolases that target the cross-links between peptidoglycan chains.
420 Therefore, the LbcA•CtpA complex might be a major control hub used by *P. aeruginosa*
421 to regulate peptidoglycan cross-link hydrolysis.

422 An exciting parallel exists between the LbcA•CtpA complex we have discovered,
423 and the NlpI•Prc complex in *E. coli*. Prc is a CTP, and NlpI is an outer membrane
424 lipoprotein with TPR motifs, and together they degrade the peptidoglycan hydrolase
425 MepS (Singh *et al.*, 2015). Therefore, the similarities between LbcA•CtpA and NlpI•Prc
426 are obvious. However, there are also important differences. Prc and CtpA are
427 evolutionarily divergent, differing in size by approximately 30 kDa and belonging to
428 different CTP subfamilies. Although NlpI and LbcA are both outer membrane
429 lipoproteins containing short TPR motifs, their primary sequences are not similar and
430 LbcA is twice the size of NlpI. Recently, the structure of the *E. coli* NlpI•Prc complex
431 was solved, showing that an NlpI homodimer binds two Prc monomers to create
432 docking sites for the MepS substrate (Su *et al.*, 2017). Although the LbcA•CtpA complex
433 in *P. aeruginosa* could have similarities to this, we suspect that its stoichiometry and
434 functioning will have differences, due to the different sizes of the proteins involved and

435 their evolutionary divergence. Regardless, it is important that two very different CTPs,
436 and two very different lipoproteins, form complexes in two significantly divergent
437 bacterial species to degrade peptidoglycan hydrolases. This suggests that this could be
438 an extremely widespread phenomenon. Therefore, we speculate that a new paradigm
439 will emerge in which many bacterial CTPs work with partner proteins, and that one of
440 their most important conserved functions will be to target cell wall hydrolases.

441 The most abundant protein trapped by the inactive LbcA•CtpA-S302A complex
442 was PA0667, which we named MepM due to its homology with *E. coli* MepM (Fig. 4B).
443 By analogy to its *E. coli* homolog, MepM is predicted to be a DD-endopeptidase that
444 cleaves the D-Ala-*m*-DAP cross-links between the peptide chains of parallel glycan
445 strands within peptidoglycan (Singh *et al.*, 2012). Our finding that LbcA•CtpA degrades
446 MepM suggests that MepM activity will increase in a Δ*ctpA* mutant. Consistent with this,
447 peptidoglycan cross-linking was reduced in the Δ*ctpA* mutant (Fig. 6), and a Δ*mepM*
448 mutation suppresses every phenotype of a Δ*ctpA* mutant we have tested (Fig. 5 and
449 data not shown). Uncovering the precise molecular explanations will need more work,
450 but increased cleavage of peptidoglycan cross-links in a Δ*ctpA* mutant might
451 compromise the cell wall, leading to inefficient T3SS function as well as altered cell
452 surface properties that cause the accelerated surface attachment phenotype.

453 Although *E. coli* Prc has been implicated in processing PBP3/FtsI (Hara *et al.*,
454 1991), MepS is the only substrate it has been convincingly shown to degrade (Singh *et*
455 *al.*, 2015). Therefore, it is not surprising that a Δ*mepS* mutation suppresses Δ*prc*
456 phenotypes in *E. coli* (Singh *et al.*, 2015). However, there is a conundrum for *P.*
457 *aeruginosa* CtpA. In addition to MepM, LbcA•CtpA degrades at least three more

458 proteins (PA1198, PA1199 and PA4404; Figs. 8 and 9). Like MepM, all are predicted to
459 be DD-endopeptidases that cleave peptidoglycan cross-links (Fig. 9). If up to four
460 peptidoglycan cross-link hydrolases can accumulate in a Δ*ctpA* mutant, why did
461 removing only one of them (MepM) suppress Δ*ctpA* phenotypes? A trivial possibility is
462 that some of these hydrolases are not synthesized and/or active in the conditions in
463 which we monitored Δ*ctpA* phenotypes. Indeed, after growth in T3SS-inducing
464 conditions, the LbcA•CtpA-S302A complex did not pull down any PA1199, and only low
465 amounts of PA4404 (2 and 4 PSMs in two independent samples, see Supplemental
466 Table 1). However, PA1198 was pulled down with comparable abundance to MepM,
467 suggesting that it had accumulated (Fig. 4B), and all four substrates accumulate in a
468 ΔctpA mutant grown in LB broth (Fig. 8A). Another intriguing possibility is that some
469 hydrolases function as part of a multi-hydrolase complex, and removing only one of
470 them destroys the function of the entire complex. The lytic transglycosylases MltD and
471 RlpA were pulled down abundantly by the LbcA•CtpA-S302A trap, but they do not
472 appear to be substrates (Figs 4B and 8A). This could be explained if they interact with
473 MepM and/or PA1198, so that they were pulled down because CtpA-S302A had
474 engaged these substrates. We have not yet been able to make null mutants of all the
475 other CtpA substrates, but addressing their role in Δ*ctpA* phenotypes, as well as
476 investigating the possibility of multi-hydrolase complexes, are exciting avenues for
477 future research.

478 The CtpA substrates MepM (PA0667) and PA4404 are in the LytM/M23 family of
479 peptidases, and both have similarity to *E. coli* MepM. However, indirect genetic
480 evidence suggests that Prc, the only CTP in *E. coli*, might not degrade MepM in that

481 species (Lai *et al.*, 2017). *E. coli* Prc does degrade the NlpC/P60 peptidase family
482 member MepS (Singh *et al.*, 2015). This is notable, because the two other substrates of
483 CtpA in *P. aeruginosa*, PA1198 and PA1199, are homologous to each other and to *E.*
484 *coli* MepS. Therefore, despite being from divergent CTP subfamilies, *P. aeruginosa*
485 CtpA and *E. coli* Prc both degrade MepS-like hydrolases. This is perhaps surprising
486 because unlike *E. coli*, *P. aeruginosa* has a second CTP, and the other one is a close
487 homolog of *E. coli* Prc (PA3257, also known as AlgO). The abundance of PA1198 and
488 PA1199 in a Δ*ctpA prc*$^+$ strain (Fig. 8A) suggests that Prc does not degrade MepS-like
489 hydrolases in *P. aeruginosa*. Another goal for future work is to address this issue
490 definitively by studying the role of *P. aeruginosa* Prc.

491 *P. aeruginosa* Prc was proposed to degrade mutant forms of antisigma factor
492 MucA in isolates from cystic fibrosis patients, causing activation of the extracytoplasmic
493 function (ECF) sigma factor AlgT/U and constitutive alginate production (Reiling *et al.*,
494 2005, Sautter *et al.*, 2012). Prc has also been linked to AlgT/U activation in strains with
495 wild type MucA (Wood *et al.*, 2006). This is intriguing because the AlgT/U regulon can
496 also be induced by cell wall-inhibitory antibiotics (Wood *et al.*, 2006). Like *P. aeruginosa*
497 CtpA, and *E. coli* Prc, it is possible that *P. aeruginosa* Prc also cleaves one or more
498 peptidoglycan modifying enzymes. Therefore, the impact of Prc on the AlgT/U regulon
499 could be a consequence of altered peptidoglycan rather than Prc cleaving MucA
500 directly. In fact, CtpA overproduction can also induce an ECF sigma factor that can be
501 activated by the cell wall-inhibitory antibiotic D-cycloserine, but CtpA is unlikely to
502 cleave its antisigma factor directly (Seo & Darwin, 2013). Prc has also been implicated
503 in activating several other ECF sigma factors in *Pseudomonas* species (Bastiaansen *et*

504 *al.*, 2014). However, induction of ECF sigma factors by cell wall stress is common, and
505 so an effect of Prc on peptidoglycan could perhaps be the explanation. Importantly, Prc
506 has not been shown to cleave any antisigma factor directly.

507 In summary, we have discovered that a binary protein complex degrades at least
508 four proteins predicted to cleave peptidoglycan cross-links in *P. aeruginosa* (Fig. 9).
509 Therefore, LbcA•CtpA might be a central hub used to control peptidoglycan hydrolysis,
510 which is a reaction with the potential for catastrophic consequences if it is not carefully
511 constrained. Similarities to the distantly related NlpI•Prc system of *E. coli* suggest that
512 this is likely to emerge as a widespread phenomenon in diverse bacteria. Given the
513 links between CTPs and virulence in other pathogens, and the importance of
514 peptidoglycan in infectious disease and its treatment, this could have major significance.
515 So far, it has been difficult to investigate when and how degradation of the LbcA•CtpA
516 substrates is regulated, because they are difficult to detect in protease-competent
517 strains (e.g. Figs. 4 and 7). However, even though CtpA and LbcA levels do not change,
518 our preliminary evidence suggests that at least one substrate might be degraded at
519 different rates depending on the growth phase, (D. Srivastava and A. J. Darwin,
520 unpublished data). Investigating how this regulation occurs, and the signal(s) involved,
521 is an exciting question for the future. Other questions include if there is any similarity
522 and/or overlap in the functions of CtpA and Prc; and what are the roles of their
523 proteolytic substrates in *P. aeruginosa* physiology and virulence.

524

525

526

527 **Materials and methods**

528 **Bacterial strains and standard growth conditions**

529 Strains and plasmids are listed in Table 1. Bacteria were grown routinely in Luria-
530 Bertani (LB) broth or on LB agar at 37˚C. During conjugation procedures, *P aeruginosa*
531 was occasionally selected for on Vogel-Bonner minimal (VBM) agar. All *P. aeruginosa*
532 strains are derivatives of strain PAK (Strom & Lory, 1986). *E. coli* K-12 strain SM10 was
533 used to conjugate plasmids into *P. aeruginosa* (Miller & Mekalanos, 1988). Antibiotics
534 were used as follows: ampicillin (200 µg/ml for *E. coli*), kanamycin (75 µg/ml for *E. coli*),
535 carbenicillin (150 µg/ml for *P. aeruginosa*), spectinomycin (50 µg/ml for *E. coli* and 500
536 µg/ml for *P. aeruginosa*), streptomycin (50 µg/ml for *E. coli* and 250 µg/ml for *P.*
537 *aeruginosa*), gentamicin (15 µg/ml for *E. coli* and 75 µg/ml for *P. aeruginosa*), and
538 Irgasan (25 µg/ml for *P. aeruginosa*).

539

540 **Plasmid and strain constructions**

541 Plasmid inserts were generated by PCR using standard methods and confirmed by
542 DNA sequencing. In frame deletion mutants were constructed using the *sacB*$^+$ suicide
543 vector, pEX18Ap (Table 1). Two fragments of ~ 500bp each corresponding to regions
544 upstream and downstream of the deletion site were amplified by PCR and cloned into
545 the pEX18Ap vector. The plasmids were integrated into the *P. aeruginosa* chromosome
546 after conjugation from *E. coli* SM10 and sucrose resistant, carbenicillin sensitive
547 segregants were isolated on LB agar containing 10% sucrose. Deletions were verified
548 by colony PCR analysis. To construct Δ*lbcA::aacC1* mutants, the *aacC1* cassette from
549 plasmid p34s-Gm (Table 1) was cloned between the upstream and downstream

550 fragments in pEX18Ap, with *aacC1* in the same orientation as the deleted *lbcA* gene.
551 Sucrose resistant, carbenicillin sensitive, and gentamycin resistant segregants were
552 isolated and verified by colony PCR analysis.

553 To make strain AJDP1140 encoding CtpA-S302A, two ~ 0.5 kb fragments
554 flanking codon 302 of *ctpA* were amplified from the *P. aeruginosa* chromosome. For
555 each fragment one of the primers incorporated a mis-match at the codon 302 region to
556 convert it to encode alanine instead of serine. The fragments were then joined in a PCR
557 SOEing reaction (Heckman & Pease, 2007) via their overlapping regions around codon
558 302. This fragment was cloned into plasmid pEX18Ap and then used to exchange for
559 the corresponding region of the native *ctpA* gene by integration, selection for sucrose-
560 resistant segregants and confirmation by colony PCR and DNA-sequencing.

561 To make strains AJDP1133 and AJDP1153 encoding CtpA-FLAG-His_6 and CtpA-
562 S302A-FLAG-His_6, respectively, two ~ 500 bp fragments surrounding the stop codon of
563 *ctpA* were amplified from the *P. aeruginosa* chromosome. For each fragment one of the
564 primers incorporated a region encoding FLAG-His_6. The fragments were then joined in a
565 PCR SOEing reaction via their overlapping FLAG-His_6 sequences. These fragments
566 were cloned into plasmid pEX18Ap and then used to fuse the FLAG-His_6 encoding
567 region to the native *ctpA* gene by integration, selection for sucrose-resistant segregants
568 and confirmation by colony PCR and DNA-sequencing of the PCR product.

569 Plasmids encoding C-terminal FLAG-tagged proteins were constructed by
570 amplifying genes from *P. aeruginosa* genomic DNA using a downstream primer that
571 incorporated a region encoding the FLAG tag, and then cloning into pHERD20T or
572 pVLT35. Plasmids for protein overproduction and purification were constructed by PCR

573 amplification of genes, without their predicted N-terminal signal sequences and stop
574 codons, and cloning into pET-24b(+) in frame to encode C-terminal His_6-tagged
575 versions.
576
577 **Polyconal antiserum production and immunoblotting**
578 *E. coli* strain ER2566 (NEB) containing a pET-24b(+) derivative encoding MepM-His_6,
579 LbcA-His_6 or OprF-His_6 was grown in LB broth to mid-log phase at 37˚C with vigorous
580 aeration. Protein production was induced with 1mM IPTG for 4 hrs at 37˚C for LbcA-His_6
581 and OprF-His_6, or overnight at 16˚C for MepM-His_6. The proteins were purified under
582 denaturing conditions by nickel-nitrilotriacetic acid (NTA) affinity chromatography as
583 described by the manufacturer (Qiagen). Polyclonal rabbit antisera were raised against
584 the proteins by Covance Research Products Inc.
585 Semi dry electroblotting was used to transfer SDS-PAGE separated samples to
586 nitrocellulose. Chemiluminescent detection was done after incubation with polyclonal
587 antiserum or monoclonal antibody, followed by goat anti-rabbit IgG (Sigma) or goat anti-
588 mouse IgG (Sigma) horseradish peroxidase conjugates used at the manufacturers
589 recommended dilution. Primary antisera or antibodies were diluted 5,000-fold for anti-
590 THE-His (GenScript) and anti-FLAG M2 (Sigma), 7,500-fold for anti-MepM, 8,000-fold
591 for anti-LbcA, 10,000-fold for anti-PA0943, anti-PA4068 and anti-CtpA (Seo *et al.*, 2009,
592 Seo & Darwin, 2013) and 20,000 fold for anti-OprF.
593
594 **CtpA-FLAG-His_6 tandem purification**
595 *P. aeruginosa* strains were inoculated into 100 ml LB broth to an optical density (OD)

596 600 nm of 0.05. The cultures were grown at 37˚C with aeration for ~ 5 h until the OD
597 600 nm was 1.2-1.4, and cells were collected by centrifuging at 6,500 x *g* for 15 min.
598 For formaldehyde cross-linking, the pellet was washed with ice cold 10 mM potassium
599 phosphate buffer, pH 8.0 and resuspended to an OD 600 nm of 5 in the same buffer.
600 1% formaldehyde was added followed by incubation at room temperature for 30 min.
601 0.3 M Tris-HCl pH 7.5 was added to quench cross-linking and the cells were collected
602 by centrifuging at 6,500 x *g* for 15 min and 4˚C for 15 min. The pellet was suspended in
603 3 ml lysis buffer (50 mM Tris-HCl pH 7.5, 150 mM NaCl, 5 mM Imidazole). Then Roche
604 complete protease inhibitors (2x concentration), 1 µg/ml DNaseI, 1 µg/ml RNase, and 1
605 mg/ml lysozyme were added. Cells were disrupted by sonication and then 1% *n*-dodecyl
606 β-D-maltoside (DDM) was added followed by incubation with rotation for 30 min at 4˚C.
607 Insoluble material was removed by centrifuging at 13,000 x *g* for 30 min at 4˚C. 200 µl
608 of nickel-NTA agarose equilibrated in lysis buffer was added to the supernatant,
609 followed by incubation with rotation for 1.5 h at 4˚C. The resin was collected in a 2 ml
610 drip column and washed with 4 ml lysis buffer, followed by 4 ml lysis buffer containing
611 20mM imidazole. Proteins were eluted with 1 ml lysis buffer containing 250 mM
612 imidazole and then mixed with 30 µl anti-FLAG M2 agarose resin (Sigma) equilibrated in
613 TBS (10 mM Tris-HCl pH 7.5, 150 mM NaCl), and incubated with rotation for 2 h at 4˚C.
614 A 1 ml spin column (Pierce catalog number 69725) was used to wash the resin three
615 times with 800 µl of TBS. Proteins were eluted by adding 100 µl of 2 µg/ml FLAG
616 peptide (F3290 Sigma) in TBS and incubating with rotation at 4˚C for 30 min. Proteins
617 present were identified by LC-mass spectrometry analysis (NYU School of Medicine
618 Proteomics Laboratory).

619 **CtpA-His$_6$, LbcA-FLAG tandem purification**

620 Δ*ctpA* strains containing pVLT35 derivatives encoding CtpA-His$_6$ or CtpA-S302A-His$_6$,
621 and pHERD20T encoding LbcA-FLAG, were inoculated to an OD 600 nm of 0.05 in 250
622 ml LB broth containing 5 mM EGTA to induce the T3SS. Culture medium also contained
623 100 μM IPTG and 0.02% (w/v) arabinose to induce protein production. The cultures
624 were incubated at 37˚C with 225 rpm rotation until the OD 600 nm was ~ 1.5. The
625 procedures described in the preceding section were used for protein purification and
626 identification.

627

628 **Analysis of T3SS substrates in cell free supernatants**

629 Strains were inoculated to an OD 600 nm of 0.04 into test tubes containing 5 ml of
630 Tryptic Soy Broth supplemented with 5 mM EGTA, and grown for 6 h at 37˚C on a roller
631 drum. Cells were removed from the equivalent of 1 ml of culture at OD 600 nm of 1.5 by
632 centrifugation at 3,300 x *g* for 15 min at 4˚C. The supernatant was filtered with a 0.22
633 μm syringe filter (Millipore) to remove any remaining cells. 1/10th volume trichloroacetic
634 acid was added to the supernatant, followed by incubation at 4˚C overnight to
635 precipitate proteins. The proteins were collected by centrifugation at 4,500 x *g* for 40
636 min at 4˚C. The pellet was washed with 1 ml ice cold acetone, then resuspended in 1 ml
637 of ice cold acetone and incubated for 1 h on ice. The proteins were collected again by
638 centrifugation at 4,500 x *g* for 40 min at 4˚C. The pellet was dried at room temperature
639 for 30-40 min until no acetone aroma remained and resuspended in SDS-PAGE sample
640 buffer containing β-mercaptoethanol. Samples was separated by SDS PAGE (12.5%
641 polyacrylamide) and proteins were visualized by staining with silver.

642 **Surface attachment assay**

643 Saturated cultures in LB broth were diluted to an OD 600 nm of 0.1 into 13 x 100 mm
644 borosilicate glass tubes containing 0.5 ml of M63 salts supplemented with 1 mM
645 $MgSO_4$, 0.5% (w/v) casamino acids and 0.2% (w/v) glucose. These cultures were
646 incubated at 30˚C without agitation for 8 h. The culture medium was removed by
647 aspiration and the tubes were washed twice with 2 ml of water. 500 µl of 0.1% (w/v)
648 crystal violet was added followed by incubation at room temperature for 10 min. The
649 crystal violet solution was removed, followed by two washes with 10 ml water, and then
650 the tubes were inverted for 10 min at room temperature prior to being photographed.
651 Finally, 1 ml of ethanol was added to dissolve the crystal violet and the absorbance of
652 this solution at 595 nm was determined. A tube that had contained the growth medium
653 alone was used to generate the blank. Each strain was tested in triplicate and the error
654 bars in the figures represent the standard deviation from the mean.

655

656 **Subcellular fractionation**

657 The osmotic shock procedure to release soluble periplasmic proteins was done as
658 described previously, except that cultures were grown to OD 600 nm of 1.0 instead of
659 1.5 (Seo & Darwin, 2013). To generate soluble and insoluble fractions from lysed cells,
660 100 ml cultures in LB broth were grown at 37˚C with shaking at 225 rpm to an OD 600
661 nm of ~ 1. Cells were collected by centrifugation and washed with 10 ml of 20 mM Tris-
662 HCl pH 7.5, 20 mM EDTA. The washed cell pellet was resuspended in 10 ml of cold 20
663 mM Tris-HCl pH 7.5, 20 mM EDTA containing Roche complete protease inhibitors. Cells
664 were lysed by two passages through a French pressure cell (1,100 psi), and intact cells

665 were removed by centrifugation at 8,000 x *g* for 10 min at 4˚C. The supernatant was
666 centrifuged at 100,000 x *g* for 1 h at 4˚C. The supernatant was retained as the soluble
667 fraction. The pellet was washed twice with 20 mM Tris-HCl pH 7.5, resuspended in 20
668 mM Tris-HCl pH 7.5 containing Roche complete protease inhibitors, and retained as the
669 membrane fraction.
670

671 **CHO-K1 cell cytotoxicity assay**

672 Chinese hamster ovary cells (CHO) were grown in Roswell Park Memorial Institute
673 (RPMI) 1640 medium supplemented with 10% fetal bovine serum (FBS) and 2 mM
674 glutamine, at 37˚C in a 5% CO_2 atmosphere. For the assay, $2x10^5$ cells/well were
675 seeded in a 24-well plate and incubated at 37˚C for 16 h. The attached cells were
676 washed with phosphate buffered saline (PBS) and then covered with RPMI 1640
677 containing 1% FBS and 2 mM glutamine. *P. aeruginosa* was grown in TSB media at
678 37˚C until the OD 600 nm was 0.8, then added to the CHO-K1 cells at a multiplicity of
679 infection of ~ 10. The 24-well plate was centrifuged at 250 x *g* for 5 min and then
680 incubated for 4 h at 37˚C. Supernatants were collected after centrifugation at 250 x *g* for
681 5 min and the lactate dehydrogenase (LDH) concentration was measured using the
682 LDH Cytotox assay (Promega) according to the manufacturer's instructions. All *P.*
683 *aeruginosa* strains were tested in triplicate.
684

685 **Cell wall isolation and digestion for LC-MS**

686 Bacteria were grown to stationary phase in 500 ml LB broth at 37 °C with 150 rpm
687 orbital shaking. The cells were harvested by centrifuging at 4,750 rpm for 20 min

688 (Allegra X-15R with SX4750 rotor, Beckman Coulter), resuspended in PBS, and
689 sterilized by immersing in a boiling water bath for 60 min. Samples were bead beat
690 (Bead Mill 24; Fisher Scientific) with 0.5 mm diameter glass beads for ten 1 min cycles
691 with 1 min rests in between. Beads and other contaminants were removed using a
692 Steriflip 20 µm nylon vacuum filter (EMD Millipore). Crude cell wall pellets were
693 resuspended in 2 ml PBS, to which 8 ml of 2% (w/v) sodium dodecyl sulfate (SDS)
694 solution was added, then placed in a boiling water bath for 60 min. Boiled cell wall
695 pellets were washed with deionized water to remove SDS and then resuspended in 2 ml
696 of 50 mM Tris pH 8.0. DNase (200 µg) was added to the cell wall suspension and
697 incubated at 37 °C for 24 h at 150 rpm, followed by addition of pronase E (200 µg) and
698 an additional 24 h incubation. Cell walls were washed once and resuspended in 1 ml of
699 50 mM Tris pH 8.0.

700 Isolated cell walls were digested by the addition of 0.5 KU of mutanolysin
701 (Sigma-Aldrich) to the cell wall suspension at room temperature and incubated for 24 h.
702 An additional 0.5 KU of mutanolysin was added to the mixture and further incubated for
703 24 h. The digested cell walls were frozen and lyophilized (Labconco) and then dissolved
704 in 1 ml of 0.375 M sodium borate buffer (pH 9.0) using HPLC-grade water. Muropeptides
705 were reduced by adding 10 mg of sodium borohydride (Fisher Scientific) at room
706 temperature for 30 min. The reduction was quenched by adding 125 µl phosphoric acid.
707 Reduced samples were frozen at -80 °C and lyophilized. Prior to LC-MS analysis,
708 lyophilized samples were resuspended in 1 ml of sample preparation buffer (1%
709 trifluroacetic acid), centrifuge filtered, and cleaned up for LC-MS using 100 µl Pierce
710 C18 tips (Thermo Scientific).

711 **Peptidoglycan analysis by liquid chromatography-mass spectrometry**

712 Mutanolysin-digested muropeptide fragments were chromatographically separated
713 using a NanoACQUITY Ultra Performance Liquid Chromatography System (Waters). A
714 reverse phase BEH C18 column (length of 100 mm and diameter of 75 μm) of 1.7 μm
715 bead with pore size of 130 Å was used. Chromatographic separation of mutanolysin-
716 digested PG was carried out by injecting 2 μl of the sample from a 5 μl sample loop to
717 the column under isocratic condition of 98% mobile phase A (0.1% formic acid in HPLC
718 water) and 2% mobile phase B (90% acetonitrile & 10% of HPLC water added with
719 0.1% formic acid) for 5 min, then a linear gradient to 50% buffer B was applied for
720 30 min for the separation. The column was regenerated under isocratic condition with
721 85% buffer B for 5 min, a linear gradient to 98% buffer A for 1 min, then isocratic at 98%
722 buffer A for 23 min. The flow rate was kept constant (0.6 μl/min) throughout the analysis.
723 Fibrinopeptide B (Glu-Fib) was used as an internal standard to correct for drift of the
724 instrument. Data were analyzed using MassLynx (Waters) and MATLAB (MathWorks).

725

726 ***In vitro* protease assay**

727 *E. coli* strain ER2566 (NEB) containing each pET-24b(+) derivative were inoculated into
728 1 L of LB broth to an OD 600 nm of 0.1. The cultures were grown at 37˚C with vigorous
729 aeration until the OD 600 nm was 0.6-0.8. Then, protein production was induced by
730 adding 1mM IPTG and incubating for 16 h at 16˚C with aeration overnight. The C-
731 terminal His_6-tagged proteins were purified under native conditions by nickel-
732 nitrilotriacetic acid (NTA) agarose affinity chromatography as recommended by the
733 manufacturer (Qiagen). Following elution with imidazole, proteins were buffer

734 exchanged into 50 mM NaH_2PO_4, 300 mM NaCl pH 8.0, using Amicon Ultra-4 centrifuge
735 filter devices (10 kDa cutoff), and then supplemented with 10% glycerol prior to storage
736 at -20˚C. For CtpA-His_6 and CtpA-S302A-His_6 only, a modification of the manufacturer's
737 recommendations was needed to improve protein purity. These two proteins were
738 eluted sequentially with 50 mM NaH_2PO_4, 300 mM NaCl, pH 8.0, containing 50 mM, 100
739 mM, 150 mM, 200 mM or 250 mM immidazole. Buffer exchange and freezing was not
740 possible with CtpA due to precipitation. Therefore, CtpA-His_6 and CtpA-S302A-His_6
741 were purified, stored at 4˚C, and used within 48 h. All experiments were done at least
742 three times with representative experiments shown in the figures.
743
744
745 **Acknowledgements**
746 We are grateful to Sindhoora Singh for constructing plasmid pAJD2003. Research
747 reported here was supported by the National Institute of Allergy and Infectious Diseases
748 (NIAID) of the National Institutes of Health, under Award Numbers R21AI117131 and
749 R01AI136901. The content is solely the responsibility of the authors and does not
750 necessarily represent the official views of the National Institutes of Health. The mass
751 spectrometric experiments for protein identification were done by the NYU School of
752 Medicine's proteomics laboratory and supported in part by NYU School of Medicine.
753 S.J.K. and B.R. conducted the peptidoglycan analysis and analyzed the data, were
754 supported by the National Institutes of Health Grant GM116130, and also acknowledge
755 the Baylor University Mass Spectrometry Centre (BU-MSC) for support.
756

References

Bandara AB, Sriranganathan N, Schurig GG & Boyle SM. 2005. Carboxyl-terminal protease regulates *Brucella suis* morphology in culture and persistence in macrophages and mice. *J Bacteriol* **187**: 5767-5775. doi: 10.1128/JB.187.16.5767-5775.2005

Bandara AB, DeShazer D, Inzana TJ, Sriranganathan N, Schurig GG & Boyle SM. 2008. A disruption of *ctpA* encoding carboxy-terminal protease attenuates *Burkholderia mallei* and induces partial protection in CD1 mice. *Microb Pathog* **45**: 207-216. doi: 10.1016/j.micpath.2008.05.005

Bastiaansen KC, Ibañez A, Ramos JL, Bitter W & Llamas MA. 2014. The Prc and RseP proteases control bacterial cell-surface signalling activity. *Environ Microbiol* **16**: 2433-2443. doi: 10.1111/1462-2920.12371

Bateman A & Bycroft M. 2000. The structure of a LysM domain from *E. coli* membrane-bound lytic murein transglycosylase D (MltD). *J Mol Biol* **299**: 1113-1119. doi: 10.1006/jmbi.2000.3778

Baumler AJ, Kusters JG, Stojiljkovic I & Heffron F. 1994. *Salmonella typhimurium* loci involved in survival within macrophages. *Infect Immun* **62**: 1623-1630. doi:

Blatch GL & Lässle M. 1999. The tetratricopeptide repeat: a structural motif mediating protein-protein interactions. *Bioessays* **21**: 932-939. doi: 10.1002/(SICI)1521-1878(199911)21:11<932::AID-BIES5>3.0.CO;2-N

Carroll RK, Rivera FE, Cavaco CK, Johnson GM, Martin D & Shaw LN. 2014. The lone S41 family C-terminal processing protease in *Staphylococcus aureus* is localized to the cell wall and contributes to virulence. *Microbiology* **160**: 1737-1748. doi: doi:10.1099/mic.0.079798-0

Chang JD, Foster EE, Thadani AN, Ramirez AJ & Kim SJ. 2017a. Inhibition of *Staphylococcus aureus* cell call biosynthesis by desleucyl-oritavancin: a quantitative peptidoglycan composition analysis by mass spectrometry. *J Bacteriol* **199**: e00278-00217. doi: 10.1128/JB.00278-17

Chang JD, Foster EE, Wallace AG & Kim SJ. 2017b. Peptidoglycan O-acetylation increases in response to vancomycin treatment in vancomycin-resistant *Enterococcus faecalis*. *Sci Rep* **7**: 46500. doi: 10.1038/srep46500

Chang JD, Foster EE, Yang H & Kim SJ. 2017c. Quantification of the d-Ala-d-Lac-terminated peptidoglycan structure in vancomycin-resistant *Enterococcus faecalis* using a combined solid-state nuclear magnetic resonance and mass spectrometry snalysis. *Biochemistry* **56**: 612-622. doi: 10.1021/acs.biochem.6b00774

Che Y, Fu A, Hou X, McDonald K, Buchanan BB, Huang W & Luan S. 2013. C-terminal processing of reaction center protein D1 is essential for the function and assembly of photosystem II in *Arabidopsis*. *Proc Natl Acad Sci USA* **110**: 16247-16252. doi: 10.1073/pnas.1313894110

Clark ST, Diaz Caballero J, Cheang M, Coburn B, Wang PW, Donaldson SL*, et al.* 2015. Phenotypic diversity within a *Pseudomonas aeruginosa* population infecting an adult with cystic fibrosis. *Sci Rep* **5**: 10932. doi: 10.1038/srep10932

de Lorenzo V, Eltis L, Kessler B & Timmis KN. 1993. Analysis of *Pseudomonas* gene products using *lacI*^{q}/*Ptrp-lac* plasmids and transposons that confer conditional phenotypes. *Gene* **123**: 17-24. doi: 10.1016/0378-1119(93)90533-9

802 Deng CY, Deng AH, Sun ST, Wang L, Wu J, Wu Y*, et al.* 2014. The periplasmic PDZ
803 domain-containing protein Prc modulates full virulence, envelops stress responses,
804 and directly interacts with dipeptidyl peptidase of *Xanthomonas oryzae* pv. *oryzae*.
805 *Mol Plant Microbe Interact* **27**: 101-112. doi: 10.1094/mpmi-08-13-0234-r
806 Dennis JJ & Zylstra GJ. 1998. Plasposons: Modular self-cloning minitransposon
807 derivatives for rapid genetic analysis of Gram-negative bacterial genomes. *Appl*
808 *Environ Microbiol* **64**: 2710-2715. doi:
809 Driscoll JA, Brody SL & Kollef MH. 2007. The epidemiology, pathogenesis and
810 treatment of *Pseudomonas aeruginosa* infections. *Drugs* **67**: 351-368. doi:
811 10.2165/00003495-200767030-00003
812 Hara H, Yamamoto Y, Higashitani A, Suzuki H & Nishimura Y. 1991. Cloning, mapping,
813 and characterization of the *Escherichia coli prc* gene, which is involved in C-terminal
814 processing of penicillin-binding protein 3. *J Bacteriol* **173**: 4799-4813. doi:
815 10.1128/jb.173.15.4799-4813.1991
816 Hauser AR. 2009. The type III secretion system of *Pseudomonas aeruginosa*: infection
817 by injection. *Nat Rev Microbiol* **7**: 654-665. doi: 10.1038/nrmicro2199
818 Heckman KL & Pease LR. 2007. Gene splicing and mutagenesis by PCR-driven overlap
819 extension. *Nat Protoc* **2**: 924-932. doi: 10.1038/nprot.2007.132
820 Hernandez SB, Ayala JA, Rico-Perez G, Garcia-del Portillo F & Casadesus J. 2013.
821 Increased bile resistance in *Salmonella enterica* mutants lacking Prc periplasmic
822 protease. *Int Microbiol* **16**: 87-92. doi: 10.2436/20.1501.01.183
823 Hoang TT, Karkhoff-Schweizer RR, Kutchma AJ & Schweizer HP. 1998. A broad-host-
824 range Flp-FRT recombination system for site-specific excision of chromosomally-
825 located DNA sequences: application for isolation of unmarked *Pseudomonas*
826 *aeruginosa* mutants. *Gene* **212**: 77-86. doi: 10.1016/S0378-1119(98)00130-9
827 Hoge R, Laschinski M, Jaeger K-E, Wilhelm S & Rosenau F. 2011. The subcellular
828 localization of a C-terminal processing protease in *Pseudomonas aeruginosa*.
829 *FEMS Microbiol Lett* **316**: 23-30. doi: 10.1111/j.1574-6968.2010.02181.x
830 Jorgenson MA, Chen Y, Yahashiri A, Popham DL & Weiss DS. 2014. The bacterial
831 septal ring protein RlpA is a lytic transglycosylase that contributes to rod shape and
832 daughter cell separation in *Pseudomonas aeruginosa*. *Mol Microbiol* **93**: 113-128.
833 doi: 10.1111/mmi.12643
834 Keiler KC, Silber KR, Downard KM, Papayannopoulos IA, Biemann K & Sauer RT.
835 1995. C-terminal specific protein degradation: activity and substrate specificity of the
836 Tsp protease. *Protein Sci* **4**: 1507-1515. doi: 10.1002/pro.5560040808
837 Keiler KC, Waller PR & Sauer RT. 1996. Role of a peptide tagging system in
838 degradation of proteins synthesized from damaged messenger RNA. *Science* **271**:
839 990-993. doi: 10.1126/science.271.5251.990
840 Kumru OS, Bunikis I, Sorokina I, Bergstrom S & Zuckert WR. 2011. Specificity and role
841 of the *Borrelia burgdorferi* CtpA protease in outer membrane protein processing. *J*
842 *Bacteriol* **193**: 5759-5765. doi: 10.1128/jb.05622-11
843 Lad SP, Yang G, Scott DA, Wang G, Nair P, Mathison J*, et al.* 2007. Chlamydial CT441
844 is a PDZ domain-containing tail-specific protease that interferes with the NF-kappaB
845 pathway of immune response. *J Bacteriol* **189**: 6619-6625. doi: 10.1128/jb.00429-07

846 Lai GC, Cho H & Bernhardt TG. 2017. The mecillinam resistome reveals a role for
847 peptidoglycan endopeptidases in stimulating cell wall synthesis in *Escherichia coli*.
848 *PLoS Genet* **13**: e1006934. doi: 10.1371/journal.pgen.1006934
849 Lee M, Hesek D, Llarrull LI, Lastochkin E, Pi H, Boggess B & Mobashery S. 2013.
850 Reactions of all *Escherichia coli* lytic transglycosylases with bacterial cell wall. *J Am*
851 *Chem Soc* **135**: 3311-3314. doi: 10.1021/ja309036q
852 Lee VT, Smith RS, Tümmler B & Lory S. 2005. Activities of *Pseudomonas aeruginosa*
853 effectors secreted by the type III secretion system in vitro and during infection. *Infect*
854 *Immun* **73**: 1695-1705. doi: 10.1128/IAI.73.3.1695-1705.2005
855 Lyczak JB, Cannon CL & Pier GB. 2000. Establishment of *Pseudomonas aeruginosa*
856 infection: lessons from a versatile opportunist. *Microbes Infect* **2**: 1051-1060. doi:
857 10.1016/S1286-4579(00)01259-4
858 Miller VL & Mekalanos JJ. 1988. A novel suicide vector and its use in construction of
859 insertion mutations: osmoregulation of outer membrane proteins and virulence
860 determinants in *Vibrio cholerae* requires *toxR*. *J Bacteriol* **170**: 2575-2583. doi:
861 10.1128/jb.170.6.2575-2583.1988
862 Mitchell SJ & Minnick MF. 1997. A carboxy-terminal processing protease gene is
863 located immediately upstream of the invasion-associated locus from *Bartonella*
864 *bacilliformis*. *Microbiology* **143**: 1221-1233. doi: 10.1099/00221287-143-4-1221
865 Moore NM & Flaws ML. 2011. Epidemiology and pathogenesis of *Pseudomonas*
866 *aeruginosa* infections. *Clin Lab Sci* **24**: 43-46. doi:
867 O'Toole GA & Kolter R. 1998. Initiation of biofilm formation in *Pseudomonas fluorescens*
868 WCS365 proceeds via multiple, convergent signalling pathways: a genetic analysis.
869 *Mol Microbiol* **28**: 449-461. doi: 10.1046/j.1365-2958.1998.00797.x
870 Qiu D, Damron FH, Mima T, Schweizer HP & Yu HD. 2008. PBAD-based shuttle
871 vectors for functional analysis of toxic and highly regulated genes in *Pseudomonas*
872 and *Burkholderia* spp. and other bacteria. *Appl Environ Microbiol* **74**: 7422-7426.
873 doi: 10.1128/AEM.01369-08
874 Rawlings ND, Barrett AJ & Bateman A. 2010. MEROPS: the peptidase database.
875 *Nucleic Acids Res* **38**: D227-233. doi: 10.1093/nar/gkp971
876 Reiling SA, Jansen JA, Henley BJ, Singh S, Chattin C, Chandler M & Rowen DW. 2005.
877 Prc protease promotes mucoidy in *mucA* mutants of *Pseudomonas aeruginosa*.
878 *Microbiology* **151**: 2251-2261. doi: 10.1099/mic.0.27772-0
879 Satoh K & Yamamoto Y. 2007. The carboxyl-terminal processing of precursor D1
880 protein of the photosystem II reaction center. *Photosynth Res* **94**: 203-215. doi:
881 10.1007/s11120-007-9191-z
882 Sautter R, Ramos D, Schneper L, Ciofu O, Wassermann T, Koh CL*, et al.* 2012. A
883 complex multilevel attack on *Pseudomonas aeruginosa algT/U* expression and
884 *algT/U* activity results in the loss of alginate production. *Gene* **498**: 242-253. doi:
885 10.1016/j.gene.2011.11.005
886 Seo J, Brencic A & Darwin AJ. 2009. Analysis of secretin-induced stress in
887 *Pseudomonas aeruginosa* suggests prevention rather than response and identifies
888 a novel protein involved in secretin function. *J Bacteriol* **191**: 898-908. doi:
889 10.1128/JB.01443-08

890 Seo J & Darwin AJ. 2013. The *Pseudomonas aeruginosa* periplasmic protease CtpA
891 can affect systems that impact its ability to mount both acute and chronic infections.
892 *Infect Immun* **81**: 4561-4570. doi: 10.1128/IAI.01035-13
893 Seoane A, Sabbaj A, McMurry LM & Levy SB. 1992. Multiple antibiotic susceptibility
894 associated with inactivation of the *prc* gene. *J Bacteriol* **174**: 7844-7847. doi:
895 10.1128/jb.174.23.7844-7847.1992
896 Silber KR, Keiler KC & Sauer RT. 1992. Tsp: a tail-specific protease that selectively
897 degrades proteins with nonpolar C termini. *Proc Natl Acad Sci U S A* **89**: 295-299.
898 doi: 10.1073/pnas.89.1.295
899 Singh SK, SaiSree L, Amrutha RN & Reddy M. 2012. Three redundant murein
900 endopeptidases catalyse an essential cleavage step in peptidoglycan synthesis of
901 *Escherichia coli* K12. *Mol Microbiol* **86**: 1036-1051. doi: 10.1111/mmi.12058
902 Singh SK, Parveen S, SaiSree L & Reddy M. 2015. Regulated proteolysis of a cross-
903 link-specific peptidoglycan hydrolase contributes to bacterial morphogenesis. *Proc*
904 *Natl Acad Sci USA* **112**: 10956-10961. doi: 10.1073/pnas.1507760112
905 Strom MS & Lory S. 1986. Cloning and expression of the pilin gene of *Pseudomonas*
906 *aeruginosa* PAK in *Escherichia coli*. *J Bacteriol* **165**: 367-372. doi:
907 10.1128/jb.165.2.367-372.1986
908 Su M-Y, Som N, Wu C-Y, Su S-C, Kuo Y-T, Ke L-C*, et al.* 2017. Structural basis of
909 adaptor-mediated protein degradation by the tail-specific PDZ-protease Prc. *Nat*
910 *Commun* **8**: 1516. doi: 10.1038/s41467-017-01697-9
911 Turner KH, Everett J, Trivedi U, Rumbaugh KP & Whiteley M. 2014. Requirements for
912 *Pseudomonas aeruginosa* acute burn and chronic surgical wound infection. *PLoS*
913 *Genet* **10**: e1004518. doi: 10.1371/journal.pgen.1004518
914 Uehara T, Dinh T & Bernhardt TG. 2009. LytM-domain factors are required for daughter
915 cell separation and rapid ampicillin-induced lysis in *Escherichia coli*. *J Bacteriol* **191**:
916 5094-5107. doi: 10.1128/JB.00505-09
917 Uehara T, Parzych KR, Dinh T & Bernhardt TG. 2010. Daughter cell separation is
918 controlled by cytokinetic ring-activated cell wall hydrolysis. *EMBO J* **29**: 1412-1422.
919 doi: 10.1038/emboj.2010.36
920 Wagner VE & Iglewski BH. 2008. *P. aeruginosa* Biofilms in CF Infection. *Clin Rev*
921 *Allergy Immunol* **35**: 124-134. doi: 10.1007/s12016-008-8079-9
922 Wang CY, Wang SW, Huang WC, Kim KS, Chang NS, Wang YH*, et al.* 2012. Prc
923 contributes to *Escherichia coli* evasion of classical complement-mediated serum
924 killing. *Infect Immun* **80**: 3399-3409. doi: 10.1128/iai.00321-12
925 Wood LF, Leech AJ & Ohman DE. 2006. Cell wall-inhibitory antibiotics activte the
926 alginate biosynthesis operon in *Pseudomonas aeruginosa*: roles of σ^{22} (AlgT) and
927 the AlgW and Prc proteases. *Mol Microbiol* **62**: 412-426. doi: 10.1111/j.1365-
928 2958.2006.05390.x
929 Wurtzel O, Yoder-Himes DR, Han K, Dandekar AA, Edelheit S, Greenberg EP*, et al.*
930 2012. The single-nucleotide resolution transcriptome of *Pseudomonas aeruginosa*
931 grown in body temperature. *PLoS Pathog* **8**: e1002945. doi:
932 10.1371/journal.ppat.1002945
933 Yakhnina AA, McManus HR & Bernhardt TG. 2015. The cell wall amidase AmiB is
934 essential for *Pseudomonas aeruginosa* cell division, drug resistance and viability.
935 *Mol Microbiol* **97**: 957-973. doi: 10.1111/mmi.13077
936

Table 1. Strains and plasmids

Name	Genotype/Features	Reference or Source
P. aeruginosa strains		
PAK [a]	wild type strain	(Strom & Lory, 1986)
AJDP566	*pscC*::pAJD1	(Seo & Darwin, 2013)
AJDP730	Δ*ctpA*	(Seo & Darwin, 2013)
AJDP1041	Δ*lbcA::aacC1*	This study
AJDP1133	Φ[*ctpA-flag-his*$_6$]	This study
AJDP1140	*ctpA-S302A*	This study
AJDP1153	Φ[*ctpA-S302A-flag-his*$_6$]	This study
AJDP1228	Δ*mepM*	This study
AJDP1229	Δ*ctpA* Δ*mepM*	This study
AJDP1230	Δ*lbcA::aacC1* Δ*mepM*	This study
Plasmids		
pHERD20T	Amp^r, pMB1 *ori*, *araBp* expression vector	(Qiu *et al.*, 2008)
pET-24b(+)	Kan^r, pMB1 *ori*, *T7p* expression vector	Novagen
pEX18Ap	Amp^r, pMB1 *ori*, *oriT*, *sacB*$^+$	(Hoang *et al.*, 1998)
pVLT35	Sm^r, Sp^r, RSF1010 *ori*, *tacp* expression vector	(de Lorenzo *et al.*, 1993)
p34s-Gm	Ap^r, *aacC1*$^+$ (Gm^r), pUC *ori*	(Dennis & Zylstra, 1998)
pAJD2290	*T7p-´ctpA-his*$_6$ in pET-24b(+)	(Seo & Darwin, 2013)
pAJD2003	*T7p-´oprF-his*$_6$ in pET-24b(+)	This study
pAJD2350	*tacp-ctpA-his6 in pVLT35*	(Seo & Darwin, 2013)
pAJD2351	*tacp-ctpA-S302A-his*$_6$ in pVLT35	(Seo & Darwin, 2013)
pAJD2226	*araBp-ctpA-his6* in pHERD20T	(Seo & Darwin, 2013)
pAJD2227	*araBp-ctpA-S302A-his*$_6$ in pHERD20T	(Seo & Darwin, 2013)
pAJD2443	*tacp-lbcA-flag* in pVLT35	This study
pAJD2653	*T7p-´lbcA-his*$_6$ in pET-24b(+)	This study
pAJD2655	*T7p-´ctpA-S302A-his*$_6$ in pET-24b(+)	This study
pAJD2779	*araBp-mepM-flag* in pHERD20T	This study
pAJD2801	*araBp-PA3623-flag* in pHERD20T	This study
pAJD2809	*T7p-´mepM-his*$_6$ in pET-24b(+)	This study
pAJD2816	*araBp-PA1812-flag* in pHERD20T	This study
pAJD2817	*araBp-PA4404-flag* in pHERD20T	This study
pAJD2818	*araBp-PA3787-flag* in pHERD20T	This study
pAJD2820	*araBp-PA1198-flag* in pHERD20T	This study
pAJD2821	*araBp-PA1199-flag* in pHERD20T	This study
pAJD2832	*T7p-´PA1198-his*$_6$ in pET-24b(+)	This study
pAJD2833	*T7p-´PA3787-his*$_6$ in pET-24b(+)	This study
pAJD2834	*T7p-´PA4404-his*$_6$ in pET-24b(+)	This study
pAJD2835	*araBp-PA0639-flag* in pHERD20T	This study
pAJD2836	*araBp-PA1844-flag* in pHERD20T	This study
pAJD2837	*araBp-PA2272-flag* in pHERD20T	This study
pAJD2839	*araBp-PA5363-flag* in pHERD20T	This study
pAJD2840	*araBp-PA5551-flag* in pHERD20T	This study
pAJD2842	*araBp-PA4418-flag* in pHERD20T	This study
pAJD2844	*T7p-´PA1199-his*$_6$ in pET-24b(+)	This study
pAJD2877	*araBp-rlpA-flag* in pHERD20T	This study

a. All *P. aeruginosa* strains are derivatives of strain PAK

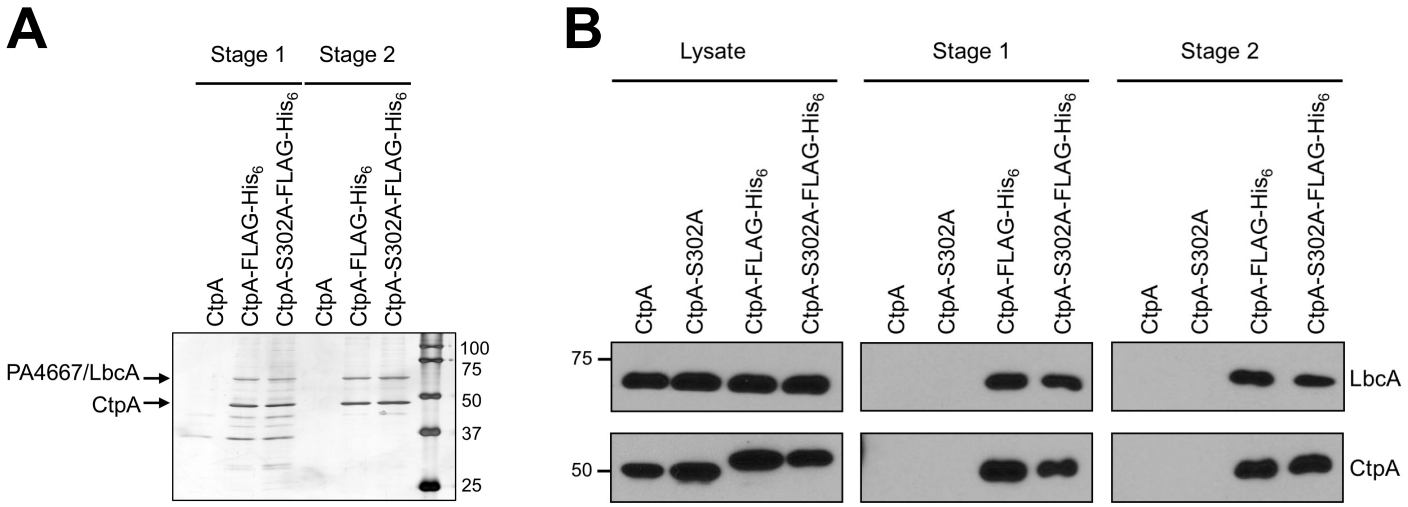

Figure 1. Identification of the CtpA interaction partner PA4667/LbcA. (A) Tandem affinity tag purification. Proteins were purified from detergent solubilized lysates of the wild type strain (CtpA), or derivatives encoding CtpA-FLAG-His_6 or the proteolytically inactive CtpA-S302A-FLAG-His_6. Purification was done with nickel agarose (Stage 1) followed by anti-FLAG M2 agarose resin (Stage 2). Samples were separated on a 12.5% SDS polyacrylamide gel, which was stained with silver. Molecular-mass-marker proteins (kDa) are labeled on the right-hand side. (B) Immunoblot analysis of detergent solubilized lysate, and Stage 1 and 2 purified samples, prepared as in panel A. LbcA and CtpA were detected with polyclonal antisera. Strains in which CtpA or CtpA-S302A were not tagged with FLAG-His_6 served as negative controls. Approximate positions of molecular-mass-marker proteins (kDa) are indicated on the left-hand side .

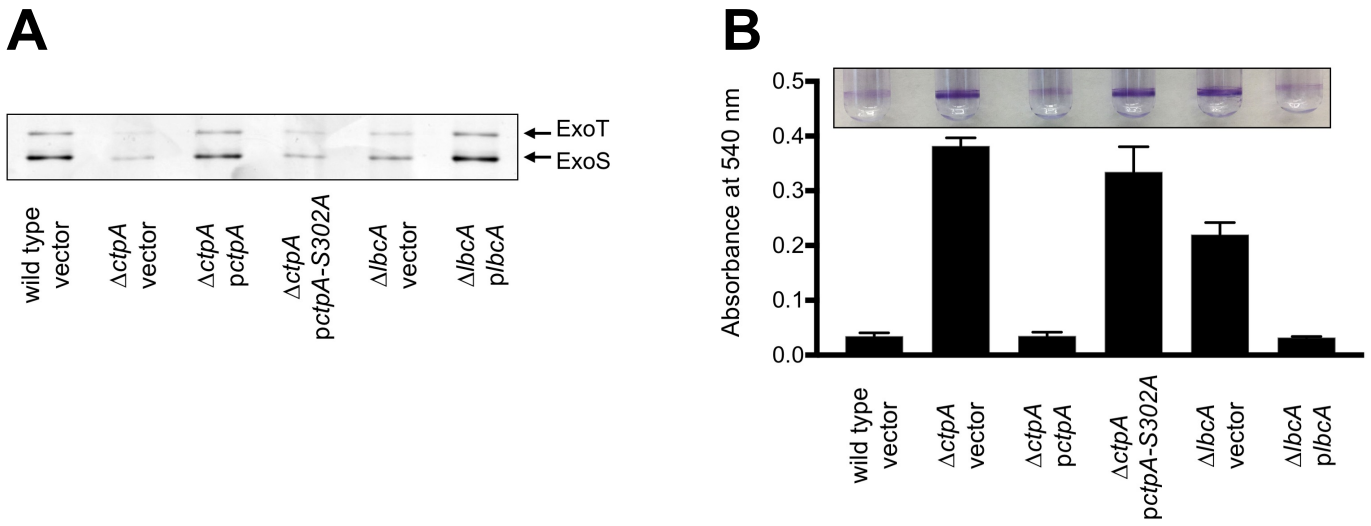

Figure 2. Δ*ctpA* and Δ*lbcA* mutants share common phenotypes. (A) T3SS function. Wild type, Δ*ctpA* or Δ*lbcA* strains contained the *tac* promoter expression plasmid pVLT35 (vector), or derivatives encoding CtpA, CtpA-S302A or LbcA as indicated. TSB growth medium contained 1mM EGTA to induce T3SS activity, and 10 μM IPTG to induce the *tac* promoter of the complementing plasmids. Cell free supernatants derived from equivalent amounts of cells were separated on a SDS-PAGE gel, which was stained with silver. The region with the abundant T3SS effectors ExoT and ExoS is shown. (B) Surface attachment. The same strains as in panel A were incubated in glass test tubes at 30°C without agitation for 8 hours. The growth medium contained 10μM IPTG to induce the *tac* promoter of the complementing plasmids. Bacterial cells attached to the glass at the air/liquid interface were stained with crystal violet (purple rings). The stain was dissolved in ethanol and quantified by measuring absorbance at 540 nm. All strains were tested in triplicate and error bars represent the standard deviation from the mean .

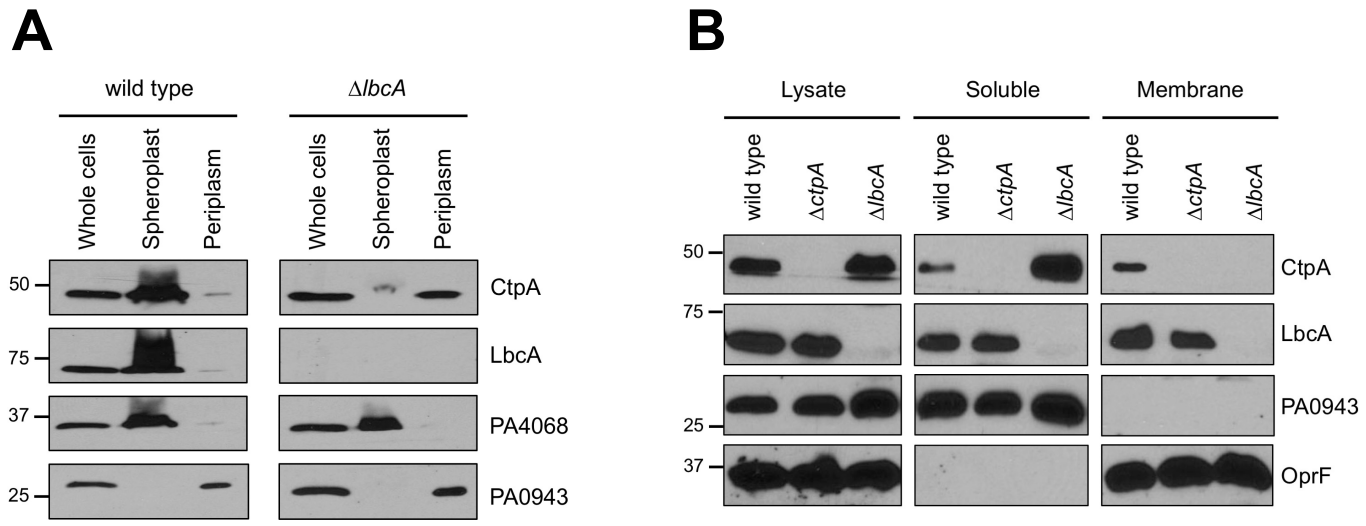

Figure 3. LbcA promotes retention of CtpA in spheroplast and membrane fractions. (A) Osmotic shock fractionation. Total cell lysate (whole cells), as well as spheroplast and periplasm fractions generated by osmotic shock, were separated by SDS-PAGE, transferred to nitrocellulose and proteins detected with polyclonal antisera. PA0943 is a soluble periplasmic protein control, and PA4068 is a cytoplasmic spheroplast-retention control (Seo & Darwin, 2013). (B) Fractionation of lysed cells. Cells were lysed by two passages through a French pressure cell and separated into soluble and insoluble (Membrane) fractions by ultracentrifugation. Samples derived from equivalent amounts of cells were separated by SDS PAGE, transferred to nitrocellulose, and proteins detected with polyclonal antisera. PA0943 is a soluble protein control and OprF is an insoluble outer membrane control.

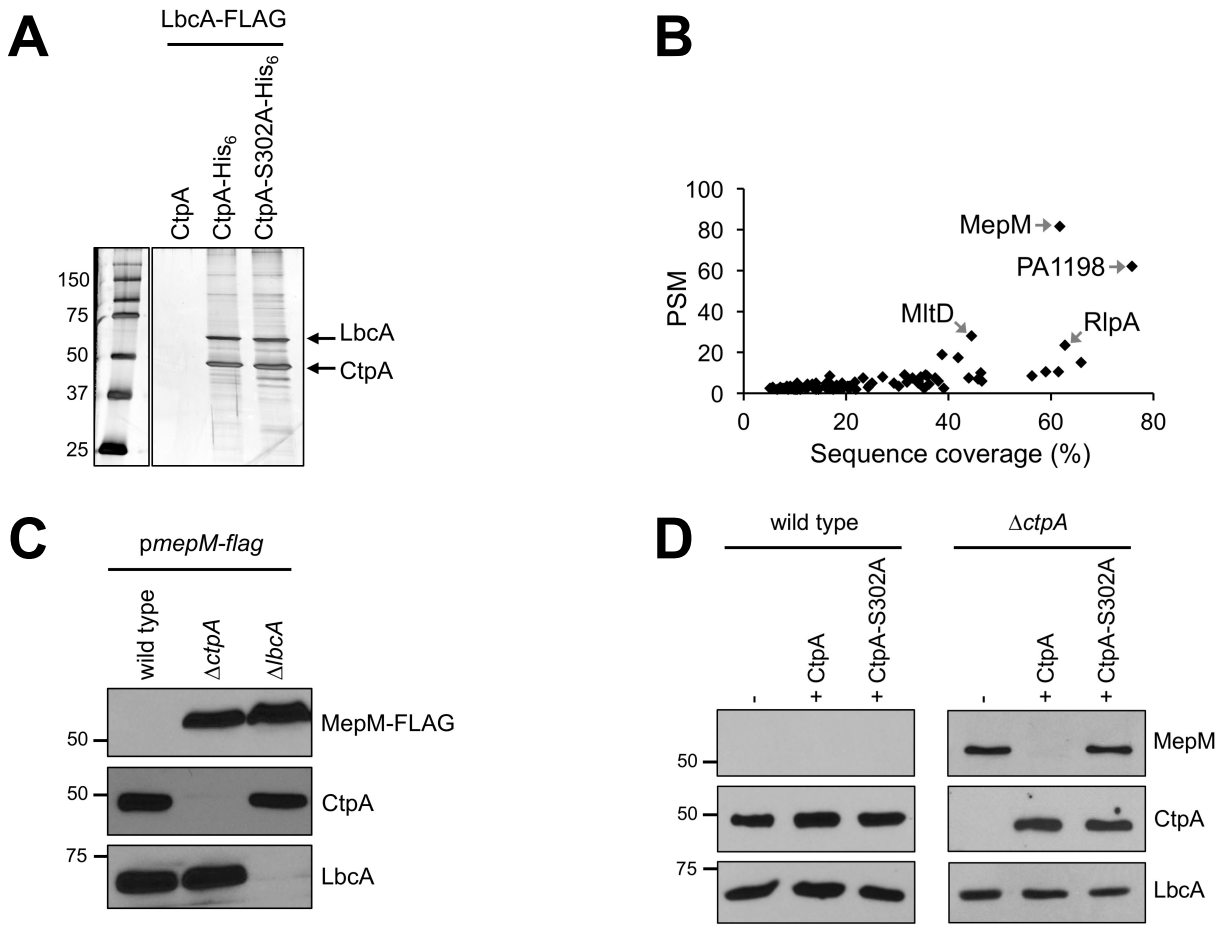

Figure 4. Identification of MepM as a putative substrate of the LbcA•CtpA proteolytic complex. (A) Tandem affinity tag purification. Proteins were purified from detergent solubilized lysates of Δ*ctpA* strains. All strains had a plasmid encoding LbcA-FLAG as well as a second plasmid encoding untagged CtpA (negative control), CtpA-His_6 or the proteolytically inactive CtpA-S302A-His_6. Purification was done with nickel agarose followed by anti-FLAG M2 agarose resin. Samples were separated on a 12.5% SDS polyacrylamide gel, which was stained with silver. Molecular-mass-marker proteins (kDa) are labeled on the left-hand side. An irrelevant region of the gel between the marker and sample lanes has been removed. (B) Scatter plot of proteins identified by mass spectrometry after purification from strains encoding CtpA-S302A-His_6. Data are the average peptide spectrum matches (PSM) and sequence coverage from duplicate purifications from strains with CtpA-S302A-His_6. Each point represents a different protein. All proteins plotted were detected in both of the LbcA•CtpA-S302A-His_6 purifications but neither of duplicate LbcA•CtpA-His_6 purifications. (C) Immunoblot analysis of equivalent amounts of whole cell lysates of wild type, Δ*ctpA* and Δ*lbcA* strains. All strains contained an arabinose-inducible expression plasmid encoding MepM-FLAG. Approximate positions of molecular-mass-marker proteins (kDa) are indicated on the left-hand side. MepM-FLAG was detected with anti-FLAG monoclonal antibodies and CtpA and LbcA were detected with polyclonal antisera. (D) Detection of endogenous MepM. Immunoblot analysis of equivalent amounts of whole cell lysates of wild type and Δ*ctpA* strains. Strains contained the *tac* promoter expression plasmid pVLT35 (-), or derivatives encoding CtpA or CtpA-S302A as indicated. Approximate positions of molecular-mass-marker proteins (kDa) are indicated on the left-hand side. MepM, CtpA and LbcA were detected with polyclonal antisera.

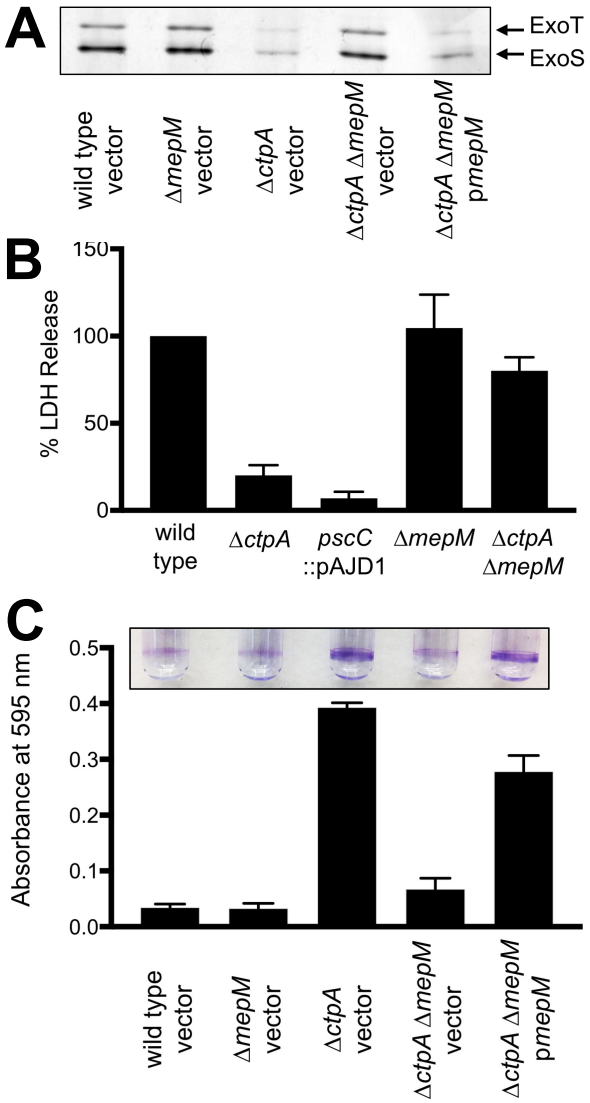

Figure 5. A *mepM* null mutation suppresses Δ*ctpA* phenotypes. (A) T3SS function. Wild type, Δ*mepM*, Δ*ctpA* or Δ*ctpA* Δ*mepM* strains contained the *araBp* promoter expression plasmid pHERD20T (vector), or a derivative encoding MepM as indicated. TSB growth medium contained 1 mM EGTA to induce T3SS activity, and 0.02% arabinose to induce the *araB* promoter of pHERD20T. Cell free supernatants derived from equivalent amounts of cells were separated by SDS-PAGE gel, which was stained with silver. The region with the abundant T3SS effectors ExoT and ExoS is shown. (B) Cytotoxicity to CHO-K1 cells. Strains with the indicated genotypes were added to CHO-K1 cells at a multiplicity of infection of ~10 and incubated for 4 h. Cell-free supernatants were then analyzed for lactate dehydrogenase (LDH) content. The amount of LDH in the supernatant following incubation with the wild type strain was set to 100% and the values for the mutants are shown as the relative percentage. Data were averaged from three independent experiments with the error bars showing the standard deviation from the mean. (C) Surface attachment. The same strains from panel A were incubated in glass test tubes at 30°C without agitation for 8 hours. The growth medium contained 0.02% arabinose to induce the *araB* promoter of the complementing plasmids. Bacterial cells attached to the glass at the air liquid interface were stained with crystal violet (purple rings). The stain was dissolved in ethanol and quantified by measuring absorbance at 595nm. All strains were tested in triplicate and error bars represent the standard deviation from the mean .

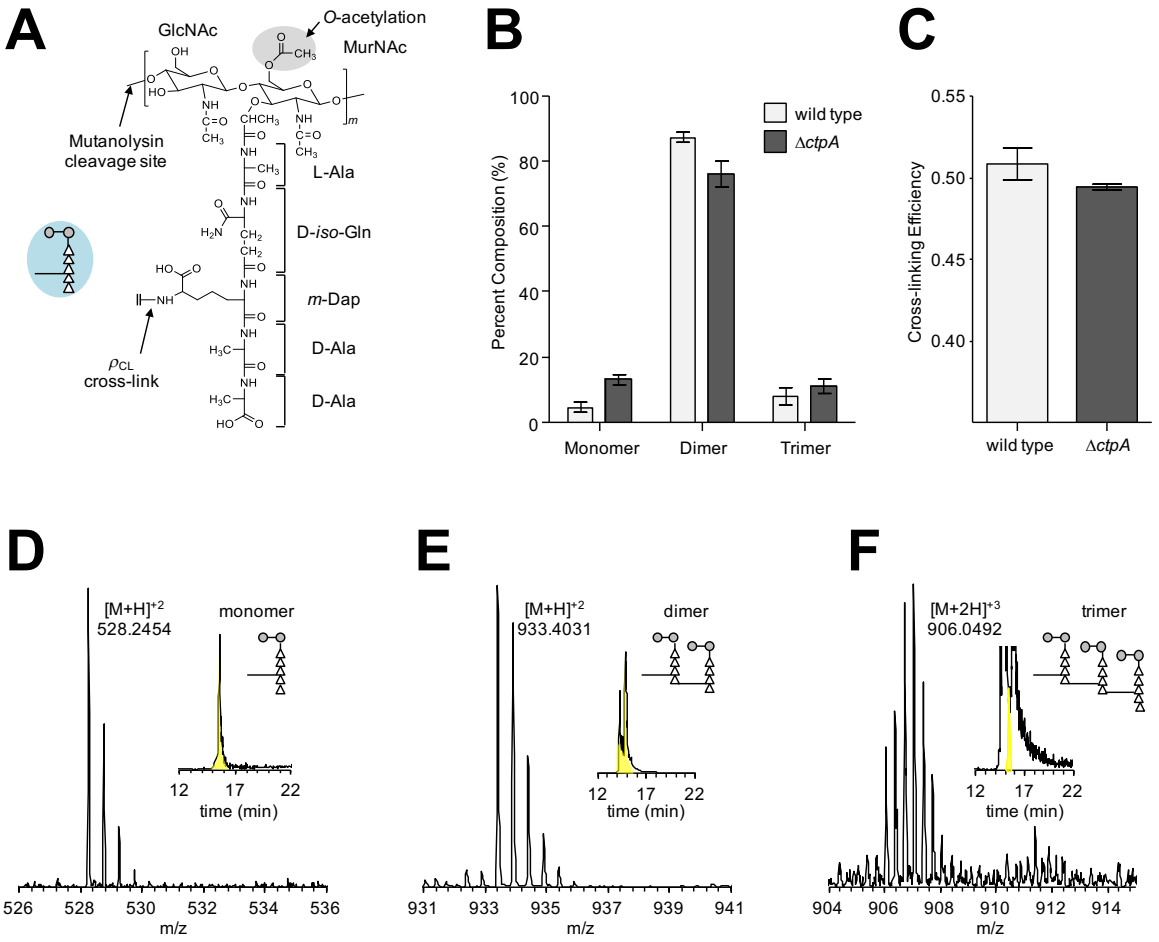

Figure 6. Changes in peptidoglycan composition of a *ΔctpA* mutant. (A) Chemical structure of peptidoglycan-repeat unit in *P. aeruginosa*. The disaccharide of peptidoglycan -repeat unit is shown with two modifications: O-acetylation of MurNAc at C6 position and amidation of D-iso-Glu in PG-stem to to D-iso-Gln. The inter-peptide bridge structure in *P. aeruginosa* is *m*-Dap. A schematic representation of a peptidoglycan-repeat unit is shown as a figure inset with the disaccharide as gray-filled circles, the amino acids in the pentapeptide stem as open triangles, and the inter-peptide bridge structure as a line. The polymerized peptidoglycans are cross-liked by forming a peptide bond between the sidechain of *m*-Dap from one repeat unit to the carbonyl carbon of penultimate D-Ala of a peptidoglycan stem from a neighboring glycan chain. (B) The mutanolysin-digested muropeptide fragments were characterized by LC-MS. Forty-seven unique muropeptide ions from the wild type and thirty-three from the *ΔctpA* mutant were identified from LC-MS and each muropeptide was quantified by integrating the extracted ion chromatogram (XIC) of the selected muropeptide ion. Peptidoglycan dimers are the most abundant muropeptides found in both wild type and *ΔctpA* mutant with percent compositions of 87.30% ± 1.34% and 75.85% ± 3.90%, respectively. Muropeptide fragments larger than trimers were not observed. The *p*-values for the differences between wild type and Δ*ctpA* strains for monomers, dimers, and trimers based on the t-test are 0.0001, 0.0003, and 0.0216, respectively. (C) The calculated peptidoglycan cross-linking efficiency (ρ_{CL}) for wild type and *ΔctpA* mutant are 50.86% ± 0.98% and 49.46% ± 0.18%, respectively, with a *p*-value of 0.0038. All errors bars represent 95% confidence interval (n = 3). Representative mass spectra of monomer (D), dimer (E), and trimer (F) are shown with the XICs as insets. The corresponding chemical structures are in Supplementary Figure S1.

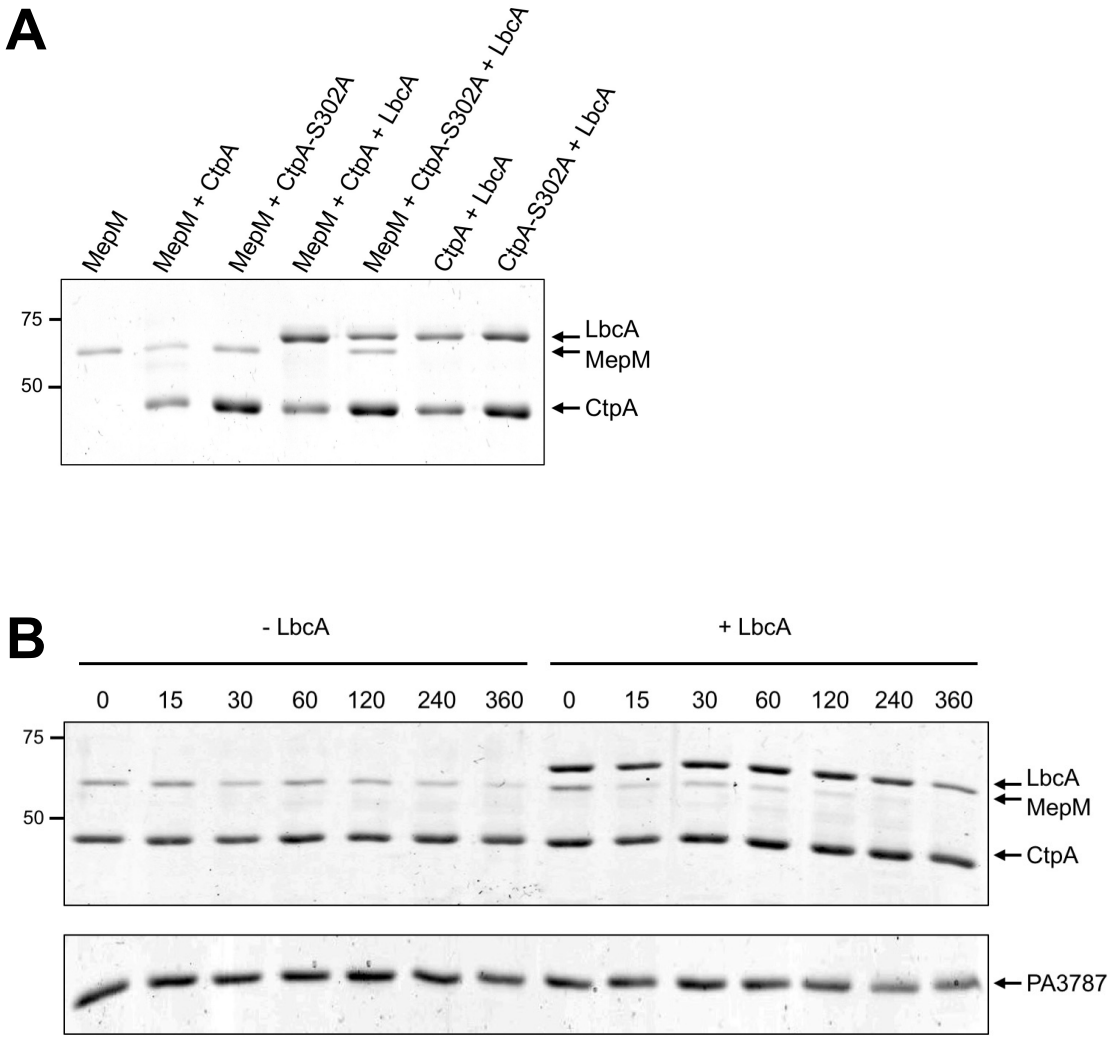

Figure 7. *In vitro* proteolysis of MepM. (A) CtpA degrades MepM and is enhanced by LbcA. 2 μM of the indicated C-terminal His_6-tagged proteins were incubated for 3 h at 37˚C. Samples were separated on a 12.5 % SDS PAGE gel, which was stained with coomassie brilliant blue. Approximate positions of molecular-mass-marker proteins (kDa) are indicated on the left-hand side. (B) Time course. Reactions contained 2 μM of CtpA-His_6 and MepM-His_6 either without (-LbcA) or with (+ LbcA) 2 μM of LbcA-His_6. Reactions were terminated at the indicated time points by adding SDS-PAGE sample buffer and boiling. As a negative control, the same experiment was done using PA3787 in place of MepM. Samples were separated on 12.5 % SDS PAGE gels, which were stained with coomassie brilliant blue. Approximate positions of molecular-mass-marker proteins (kDa) are indicated on the left-hand side. PA3787 ran at the midway point between marker proteins of 25 and 37 kDa, which were below and above the region of the gel shown in the figure.

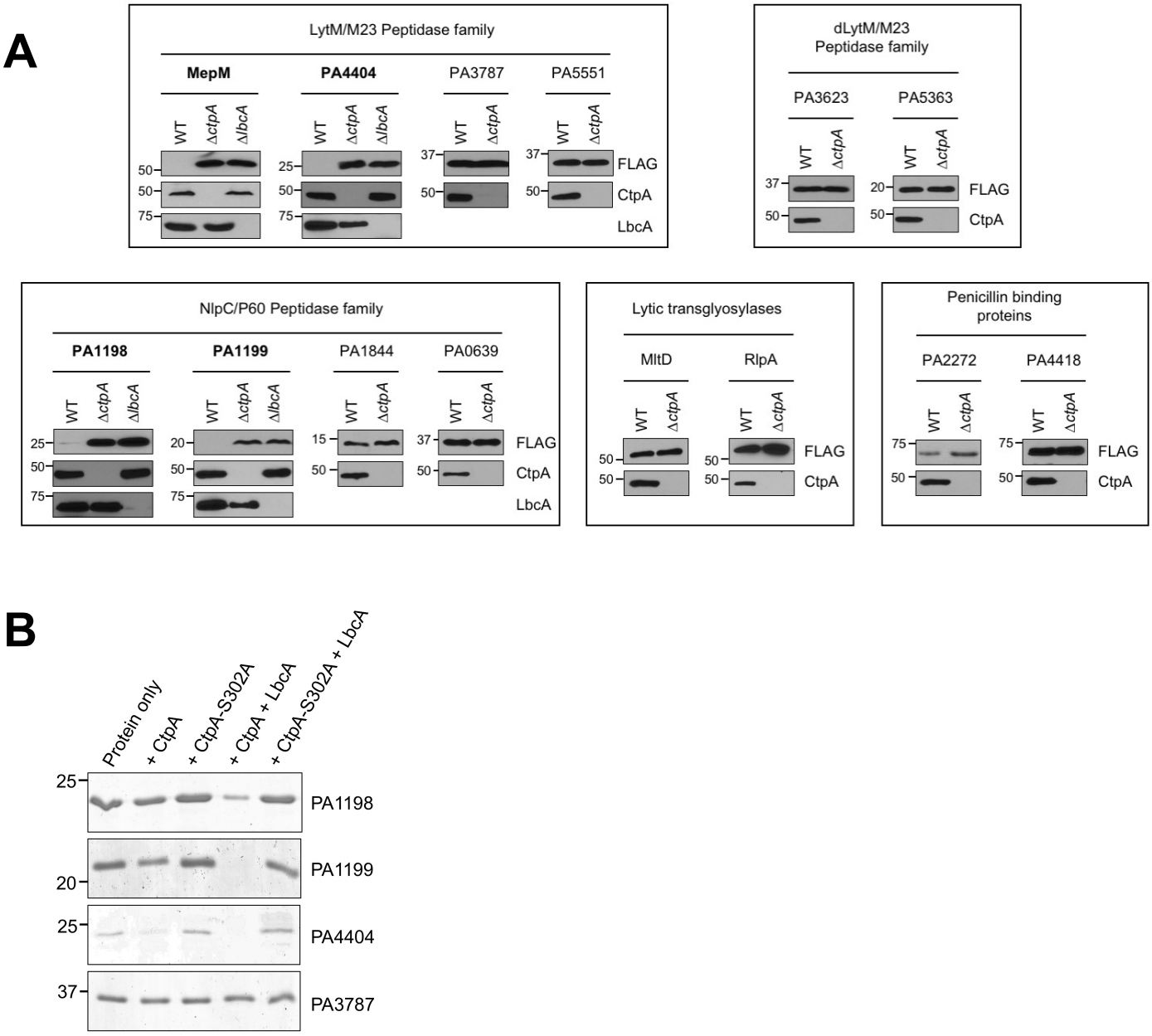

Figure 8. Identification of additional substrates of the LbcA•CtpA complex. (A) *In vivo* analysis. Immunoblot analysis of equivalent amounts of whole cell lysates of wild type and Δ*ctpA* strains, and also of Δ*lbcA* strains for proteins that accumulated in the Δ*ctpA* mutant. All strains contained an arabinose-inducible expression plasmid encoding C-terminal FLAG-tagged versions of the indicated proteins. Approximate positions of molecular-mass-marker proteins (kDa) are indicated on the left-hand side. Test proteins were detected with anti-FLAG monoclonal antibodies, and CtpA and LbcA were detected with polyclonal antisera. Each box has analysis of proteins in related families, as indicated at the top. Only those proteins with names in bold face accumulated in the Δ*ctpA* mutant. (B) *In vitro* analysis. 2 μM of the indicated C-terminal His_6-tagged proteins were incubated for 3 h at 37˚C. Protein only indicates incubation of the test substrate alone. PA3787-His_6 was used as a negative control. Samples were separated on a 15 % SDS PAGE gel, which was stained with coomassie brilliant blue. Approximate positions of molecular-mass-marker proteins (kDa) are indicated on the left-hand side .

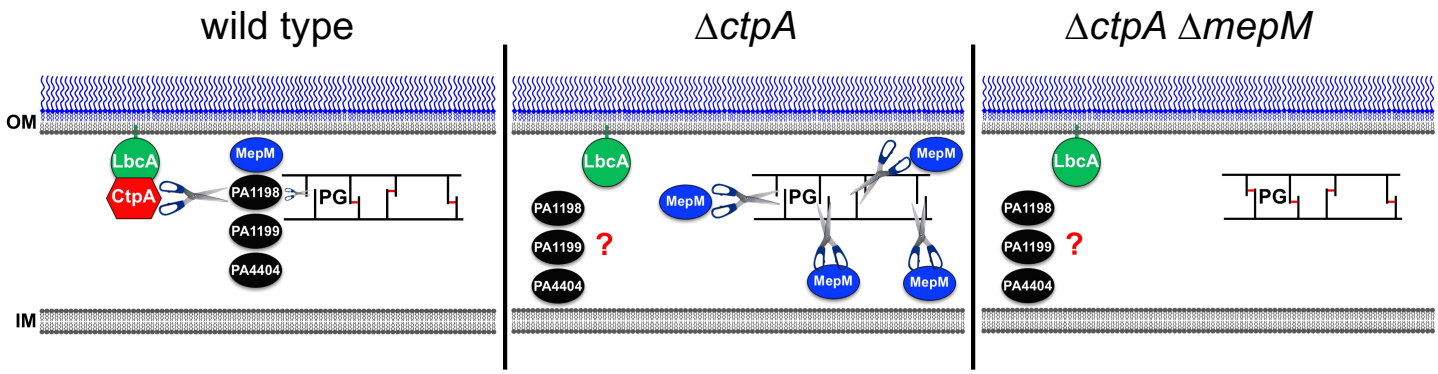

Figure 9. Model: the LbcA•CtpA complex is an important control hub for peptidoglycan cross-link hydrolases. In a wild type strain CtpA forms a complex with the outer membrane lipoprotein LbcA, which is required for CtpA to degrade its targets. The LbcA•CtpA complex has the potential to degrade at least four enzymes predicted to cleave peptidoglycan cross-links (MepM, PA1198, PA1199 and PA4404). This results in crosslink hydrolysis being carefully constrained to limit it to the amount needed for cell elongation and/or division. In a Δ*ctpA* mutant, the activity of MepM accumulates, which might cause excessive crosslink cleavage and subsequent phenotypes, including a defective T3SS and enhanced surface attachment. However, if *mepM* is deleted from the Δ*ctpA* mutant, the excessive crosslink cleavage is reduced and phenotypes revert back to wild type. It is not yet known if the PA1198, PA1199 and PA4404 substrates make any contribution to Δ*ctpA* mutant phenotypes described in this study. OM = outer membrane, IM = inner membrane.